Nuclear Physics B146 (1978) 327–367

PARTIAL-WAVE ANALYSIS OF $\bar{K}N \to \bar{K}^*N$ BETWEEN 1830 AND 2170 MeV c.m. ENERGY INCLUDING NEW DATA BELOW 1960 MeV

Rutherford Laboratory-Imperial College Collaboration

W. CAMERON, B. FRANEK, G.P. GOPAL, G.E. KALMUS, A.C. McPHERSON and R.T. ROSS [+]
Rutherford Laboratory, Chilton, Didcot, UK

T.C. BACON, I. BUTTERWORTH, R.W.M. HUGHES, P. NEWHAM and R.A. STERN
Imperial College, London, UK

Received 25 July 1978

We present data for the single-pion production final states $\bar{K}^0\pi^-p$, $K^-\pi^0p$ and $K^-\pi^+n$ from K^-p interactions at 11 c.m. energies between 1775 and 1957 MeV. Using the $K^0\pi^-p$ events the branching ratio ($K_S^0 \to \pi^+\pi^-/K_S^0 \to$ all) has been determined to be 0.657 ± 0.011. New values have also been determined for the masses and widths of the K^{*0} (890) and the K^{*-} (890). These give a value of 1.5 ± 1.5 MeV for the electromagnetic mass splitting of the K^*. Differential cross sections and the spin-density matrix elements have been extracted for the reactions $K^-p \to K^{*-}p$ and $K^-p \to \bar{K}^{*0}n$. An energy dependent partial-wave analysis of the $\bar{K}^*N$ channel from threshold up to 2170 MeV c.m. energy has been carried out yielding values for 17 resonant amplitudes for the expected Y^*'s and a new resonance, the S01(2030).

1. Introduction

The reactions

$$K^-p \to \bar{K}^0\pi^-p\,, \tag{1a}$$

$$K^-\pi^0p\,, \tag{1b}$$

$$K^-\pi^+n\,, \tag{1c}$$

have been studied at eleven approximately equally spaced incident momenta between

[+] Present address: University of Michigan, Physics Department, Ann Arbor, Michigan 48104, USA.

0.96 and 1.355 GeV/c as described in sect. 2. The contributions of the quasi-two-body reactions

$$K^- p \to K^{*-}(890)\, p\,, \tag{2a}$$

$$\to \overline{K^{*0}}(890)\, n\,, \tag{2b}$$

to these reactions and the resulting differential cross sections and differential density matrix elements have been extracted as described in sect. 3 using a four-variable fitting technique.

These new data have been combined with those previously reported for the same reactions between 1.263 and 1.843 GeV/c by a College de France-Rutherford Laboratory-Saclay-Strasbourg Collaboration [1] * and those for the reaction

$$K^- n \to K^{*-} n \tag{3}$$

extracted from the $K^0\pi^-n$ final state by the Birmingham group [2] in the range between 1800 and 2200 MeV. An energy dependent partial-wave analysis has been carried out between 1830 and 2170 MeV c.m. energy and is described in sect. 4. The implications of the results of this analysis are discussed in sect. 5.

2. New data

New data from the reactions (1a–c) have been obtained from exposures of the CERN 2m HBC to a separated K^- beam at 11 approximately equally spaced incident momenta between 0.96 and 1.355 GeV/c. Details of the exposure, scanning and measuring, beam calibration and cross-section normalisation have been published elsewhere [3].

Events of the two-prong topology provide the main contribution to the three reactions (1a–c). For this topology kinematic ambiguities were readily resolved by ionisation measurements. Events from reaction (1b) with a K^- decay were unambiguously identified. Events where the negative track decays and the positive track is identified to be a pion usually fit both the K^- decay hypothesis, reaction (1c), and the Σ^- decay hypothesis $K^- p \to \Sigma^- \pi^+ \pi^0$. On short decay tracks, measured ionisation information does not help to distinguish between the two hypotheses. For these events the Σ^- decay hypothesis was preferred on the grounds of decay probability. However the proper time distribution of all decaying negative tracks defined as K^- by the above procedures still shows an appreciable contamination from Σ^- decay events that had failed to fit as such. Events were therefore accepted as belonging to reaction (1c) and appropriately weighted, if the fit to the Σ^- decay hypothesis was unsuccessful and if the proper length for K^- decay was greater than 6.0 cm.

* Data summary tapes for the reactions $K^- p \to \bar{K} N \pi$ were made available to us by the CRSS Collaboration. These were analysed using methods described for the present data.

Two-prong events with a seen neutral decay provide a large contribution (6209 events) to reaction (1a). The K^0_S mean life-time (τ) has been determined using events having a K^0_S projected length between 0.3 cm and 8.0 cm. By maximising the likelihood function

$$\mathcal{L} = \prod_{i=1}^{N} \frac{1}{\tau} \frac{\exp[-(t_i - t_i^{\min})/\tau]}{1 - \exp[-(t_i^{\max} - t_i^{\min})/\tau]}, \tag{4}$$

where $t_i^{\min}$ and $t_i^{\max}$ are time limits, for the ith event, corresponding to the minimum and maximum projected lengths, a value for τ of $(0.891 \pm 0.017) \times 10^{-10}$ sec is obtained. This is in excellent agreement with the averaged value of $(0.893 \pm 0.002) \times 10^{-10}$ sec obtained from the post-1971 experiments [4].

Comparing the number of events fitting reaction (1a) in which the K^0 decay is seen (5702 after cuts) with the number in which it is not, the $K^0_S \to \pi^+\pi^-$ branching ratio is calculated to be 0.657 ± 0.011. This is in satisfactory agreement with the previous best determination [5] of 0.67 ± 0.01.

A total of 22 818 events were assigned to reaction (1a), 16 162 to (1b) and 19 807 to (1c). A more complete discussion of the experimental details for all three reactions can be found in ref. [6]. The values of the cross sections determined for reactions (1a–c) after correcting for scanning and through-put losses are given in table 1 and shown in fig. 1 together with previously published values [7,8]. There is general agreement with earlier data for reactions (1a) and (1b). The cross section obtained for reaction (1c) shows an almost linear increase with momentum over this energy range. There is some disagreement with values reported by the Chicago-Heidelberg Collaboration [8] at incident K^- momenta around 1.05 GeV/c.

Sample Dalitz plots together with their projections are shown in fig. 2, for each of the three reactions. The prominent features to be seen are a band corresponding to the $K^*(890)$ in all three reactions and a $\Lambda(1520)$ band in reaction (1b). A partial-wave analysis of the $\pi^0\Lambda(1520)$ channel has been reported elsewhere [9].

The $K\pi$ mass-squared distributions in the region of the $K^*(890)$ ($0.675 \leqslant M^2(K\pi) \leqslant 0.925$ (GeV/c^2)^2, a total of 50 bins) obtained by adding up data from all incident K^- momenta above 1.1 GeV/c for each of the three reactions are shown in fig. 3. Each distribution was fitted by a relativisitic Breit-Wigner shape [10] with energy independent width superimposed on a third-order polynomial background to determine the mass and width of the K^*. The parameter values obtained for the three channels are given in table 2 along with the world averages from ref. [4]. The errors quoted, in addition to the statistical uncertainties, include the effect of different background parametrisation, binning and mass range fitted.

It should be noted that whereas our values for the mass and width of the K^{*-} are consistent with the world average values, the mass of the $\overline{K^{*0}}$ is found to be almost six standard deviations lower than the present world average value. The possibility of biases in the treatment of the $K^-\pi^+$n channel has been investigated as follows

Table 1
Values of the cross sections for each $\bar{K}\pi N$ final state and for processes contributing to it: (a) $\bar{K}^0\pi^-p$; (b) $K^-\pi^0p$; (c) $K^-\pi^+n$

a

Beam Momentum in GeV/c	C.M. Energy in GeV	$\sigma[K^{*-}(890)p]$ mb	$\sigma[\bar{K}^0\Delta^0(1233)]$ mb	$\sigma[\pi^-\Sigma^+(1775)]$ mb	$\sigma[\bar{K}^0n$ LIPS] mb	$\sigma(K^-p\to\bar{K}^0\pi^-p)$ mb
0.960	1.775	0.129 ± 0.016	0.176 ± 0.018		0.192 ± 0.021	0.496 ± 0.034
1.005	1.796	0.185 ± 0.023	0.242 ± 0.024		0.229 ± 0.026	0.656 ± 0.043
1.045	1.815	0.315 ± 0.023	0.243 ± 0.018		0.406 ± 0.030	0.964 ± 0.047
1.085	1.833	0.586 ± 0.035	0.166 ± 0.013		0.502 ± 0.037	1.254 ± 0.059
1.125	1.852	1.034 ± 0.048	0.272 ± 0.019		0.350 ± 0.026	1.646 ± 0.068
1.165	1.870	1.199 ± 0.050	0.198 ± 0.013		0.394 ± 0.027	1.791 ± 0.069
1.205	1.889	1.175 ± 0.049	0.259 ± 0.016		0.378 ± 0.024	1.812 ± 0.069
1.245	1.907	1.195 ± 0.045	0.199 ± 0.011	0.010 ± 0.010	0.414 ± 0.019	1.818 ± 0.063
1.285	1.926	1.232 ± 0.046	0.252 ± 0.015	0.042 ± 0.010	0.293 ± 0.012	1.824 ± 0.060
1.320	1.941	1.108 ± 0.045	0.327 ± 0.018	0.049 ± 0.010	0.164 ± 0.012	1.648 ± 0.061
1.355	1.957	1.188 ± 0.041	0.276 ± 0.014	0.040 ± 0.010	0.252 ± 0.014	1.756 ± 0.057

b

Beam Momentum in GeV/c	C.M. Energy in GeV	$\sigma[K^{*-}(890)p]$ mb	$\sigma[\pi^0\Lambda(1520)]$ mb	$\sigma[K^-\Delta^+(1233)]$ mb	$\sigma[\pi^0\Lambda(1690)]$ mb	$\sigma[\pi^0\Sigma^0(1775)]$ mb	$\sigma[\pi^0K^-p$ LIPS] mb	$\sigma(K^-p\to K^-p\pi^0)$ mb
0.960	1.775	0.054 ± 0.007	0.656 ± 0.038	0.140 ± 0.012			0.083 ± 0.014	0.933 ± 0.049
1.005	1.796	0.087 ± 0.010	0.550 ± 0.036	0.230 ± 0.019			0.098 ± 0.017	0.965 ± 0.052
1.045	1.815	0.154 ± 0.012	0.417 ± 0.024	0.255 ± 0.016			0.282 ± 0.017	1.107 ± 0.047
1.085	1.833	0.273 ± 0.019	0.298 ± 0.021	0.339 ± 0.021			0.169 ± 0.020	1.078 ± 0.048
1.125	1.852	0.506 ± 0.027	0.287 ± 0.020	0.406 ± 0.023	0.049 ± 0.010		0.056 ± 0.011	1.304 ± 0.051
1.165	1.870	0.585 ± 0.027	0.224 ± 0.015	0.286 ± 0.020	0.044 ± 0.018		0.063 ± 0.019	1.301 ± 0.047
1.205	1.889	0.650 ± 0.028	0.180 ± 0.013	0.292 ± 0.016	0.109 ± 0.014		0.071 ± 0.011	1.302 ± 0.047
1.245	1.907	0.627 ± 0.024	0.160 ± 0.011	0.315 ± 0.014	0.089 ± 0.019		0.097 ± 0.011	1.288 ± 0.041
1.285	1.926	0.625 ± 0.024	0.209 ± 0.013	0.345 ± 0.015	0.040 ± 0.005	0.096 ± 0.006	0.019 ± 0.006	1.334 ± 0.041
1.320	1.941	0.547 ± 0.023	0.178 ± 0.013	0.256 ± 0.012	0.043 ± 0.005	0.145 ± 0.015	0.017 ± 0.006	1.185 ± 0.040
1.355	1.957	0.629 ± 0.021	0.212 ± 0.012	0.302 ± 0.012	0.045 ± 0.005	0.184 ± 0.015	0.041 ± 0.010	1.413 ± 0.039

c

Beam Momentum in GeV/c	C.M. Energy in GeV	$\sigma[\bar{K}^{*0}(890)n]$ mb	$\sigma[K^-\Delta^+(1233)]$ mb	$\sigma[\pi^+\Sigma^-(1775)]$ mb	$\sigma[K^-\pi^+n$ LIPS] mb	$\sigma(K^-p\to K^-\pi^+n)$ mb
0.960	1.775	0.129 ± 0.014	0.209 ± 0.019		0.170 ± 0.019	0.508 ± 0.033
1.005	1.796	0.131 ± 0.015	0.216 ± 0.019		0.286 ± 0.027	0.633 ± 0.040
1.045	1.815	0.279 ± 0.019	0.257 ± 0.017		0.289 ± 0.021	0.825 ± 0.039
1.085	1.833	0.355 ± 0.022	0.292 ± 0.018		0.381 ± 0.026	1.028 ± 0.047
1.125	1.852	0.560 ± 0.029	0.326 ± 0.018		0.300 ± 0.020	1.186 ± 0.048
1.165	1.870	0.725 ± 0.031	0.266 ± 0.014		0.318 ± 0.019	1.309 ± 0.047
1.205	1.889	0.865 ± 0.035	0.338 ± 0.017		0.335 ± 0.020	1.538 ± 0.053
1.245	1.907	1.153 ± 0.037	0.303 ± 0.013	0.081 ± 0.010	0.261 ± 0.013	1.798 ± 0.052
1.285	1.926	1.240 ± 0.039	0.340 ± 0.014	0.079 ± 0.010	0.172 ± 0.010	1.831 ± 0.052
1.320	1.941	1.363 ± 0.045	0.336 ± 0.016	0.117 ± 0.010	0.143 ± 0.010	1.959 ± 0.060
1.355	1.957	1.549 ± 0.043	0.348 ± 0.015	0.164 ± 0.010	0.098 ± 0.010	2.159 ± 0.055

(a) The stretch functions for $1/p$, λ and ϕ for the outgoing K^- and π^+ are found to be normal.

(b) The values, for the mass and width of the $\overline{K^{*0}}$, determined using either the measured or fitted values for the K^- and π^+ momentum vectors are found to be consistent within one standard deviation.

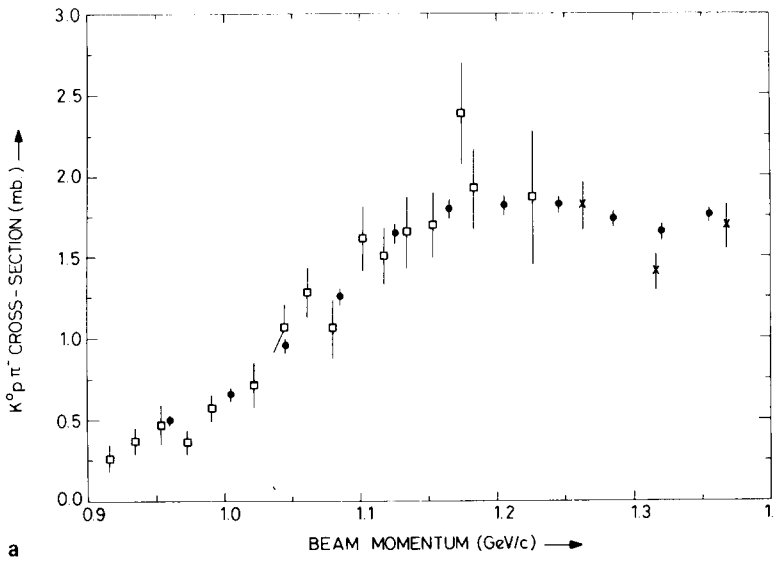

a

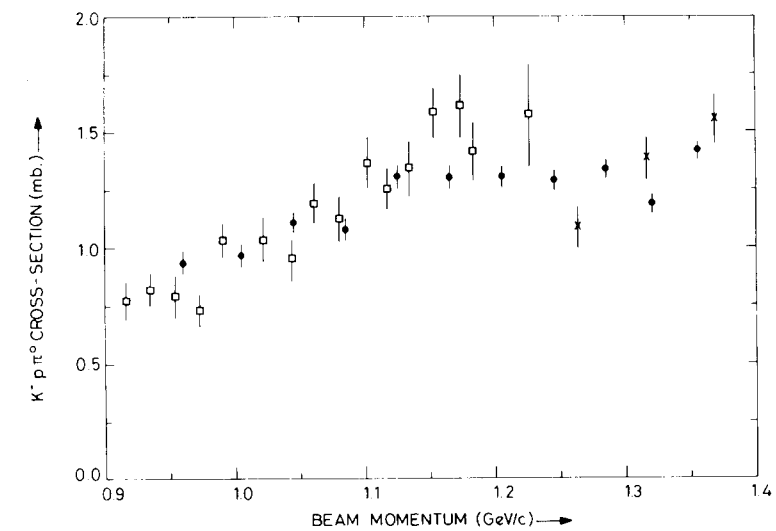

b

Fig. 1.

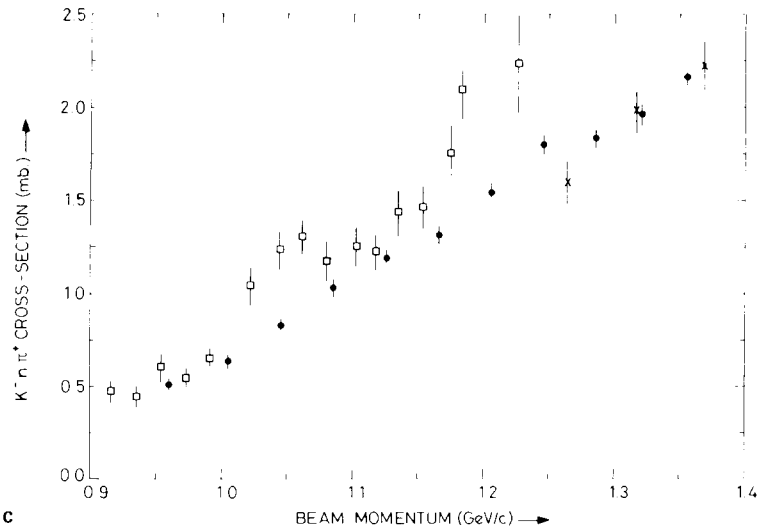

Fig. 1. $K^-p \to \bar{K}\pi N$ cross sections as a function of incident momentum: (a) $\bar{K}^0 p\pi^-$; (b) $K^-p\pi^0$; (c) $K^-n\pi^+$. The data from the present experiment is shown by ♦, the CRSS data by ✳ and the data from the CH experiment by ϕ.

(c) Separate fits to the $M^2(K^-\pi^+)$ distribution at each of the top six energies (covering a range from one to three widths above threshold) give mass and width values consistent with those from the combined data.

(d) As stated above the effects of using different orders of polynomial background and various parametrisations for the energy dependence of the K^* width have already been included in the errors quoted in table 2. The parameter values given are the ones from the best fit (with energy independent width and third-order background) to the data in each charge state.

(e) Finally, as an overall confirmation of lack of biases in invariant mass distribution we note that the value of the K^0 mass obtained from a sample of 5000 neutral $\pi^+\pi^-$ decays is consistent with the world average value.

The present experiment, therefore gives $\Delta M = M(\bar{K}^{*0}) - M(K^{*-}) = 1.5 \pm 1.5$ MeV for the electromagnetic mass difference of the K^*. It is interesting to note that this value is now consistent with a theoretical prediction of $\Delta M \leqslant 1.9$ MeV derived from a 'standard' gauge model [11] of weak, electromagnetic and strong interactions.

Similarly the $M^2(K^-p)$ distribution for reaction (1b) in the region of the $\Lambda(1520)$ was fitted to determine the mass and width of this resonance. The values obtained are reported elsewhere [9]. The $\Delta^+(1233)$ is almost as broad as the available phase space at any given incident energy in this region. It is therefore not possible to determine meaningful values for its parameters from the present data. For the 4-variable

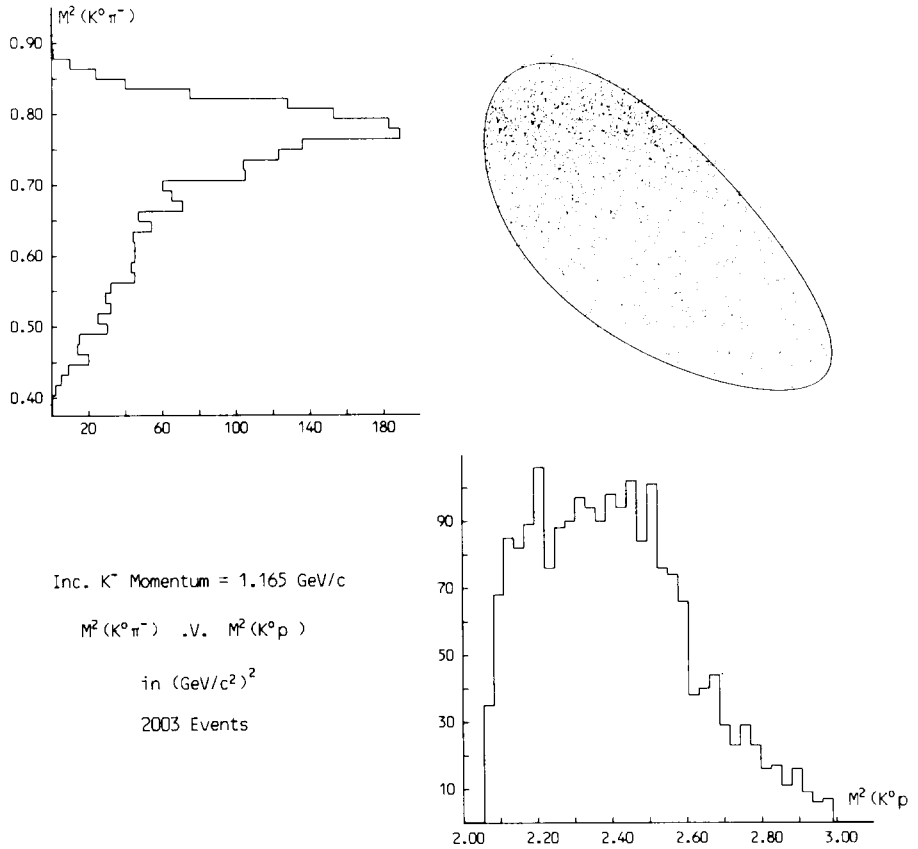

Fig. 2. Dalitz plots ($M^2(\bar{K}\pi)$ *versus* M^2 ($\bar{K}N$)) and projections for $\bar{K}^0\pi^-$p: (a) at 1.165 GeV/*c*; (b) at 1.355 GeV/*c*. For $K^-\pi^0$p: (c) at 1.205 GeV/*c*; (d) at 1.320 GeV/*c*. For $K^-\pi^+$n: (e) at 1.165 GeV/*c*; (f) at 1.355 GeV/*c*.

Table 2
Masses and widths of the $\bar{K}^*(890)^0$

Channel	Number of events above background	χ^2/Degrees of freedom	Mass$_2$ (MeV/c^2)	Width$_2$ (MeV/c^2)	Weighted Mean Values This experiment		Particle Data Table Values	
					M	Γ	M	Γ
$K^{*-} \cdot K^-\pi^+$	6,323	50.1/45	890.9±1.1	48.8±2.8	890.0±0.8	45.8±2.5	892.19±0.51	49.4±1.8
$K^{*-} \cdot \bar{K}^0\pi^-$	10,095	46.1/45	889.3±0.8	43.7±2.0				
$\bar{K}^{*0} \cdot K^-\pi^+$	10,479	35.5/45	891.5±0.8	45.2±0.8	891.5±0.8	45.2±2.0	896.12±0.33	49.9±1.1

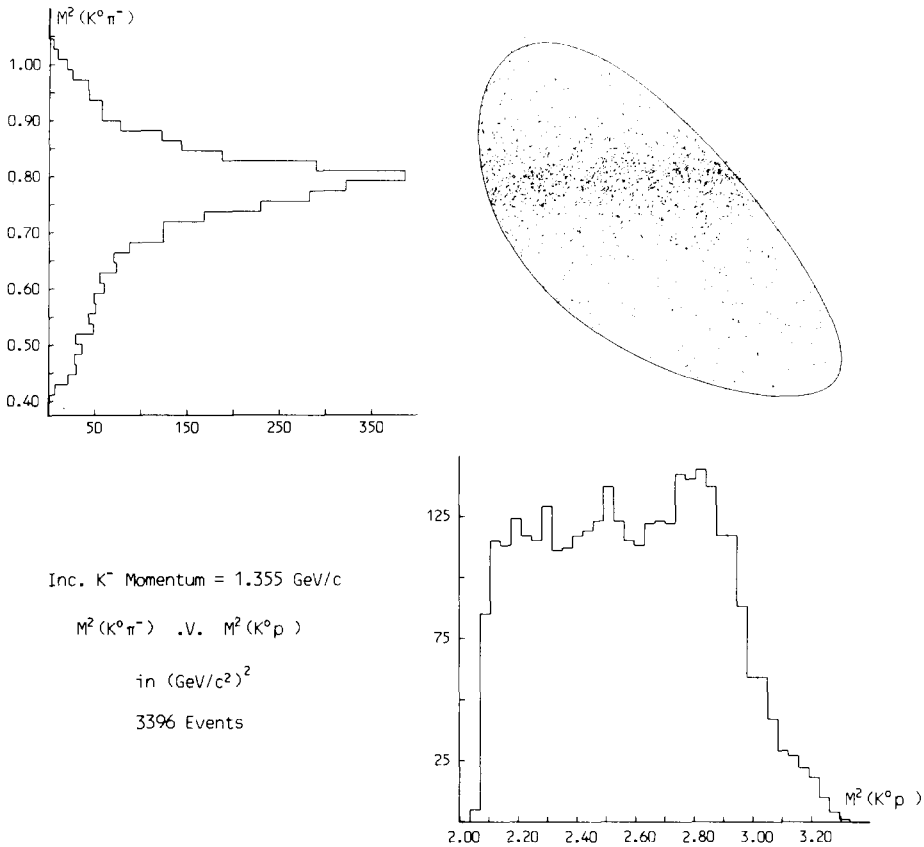

Fig. 2b.

fits, described in sect. 3 we have used the masses and widths given in ref. [4] for the Δ and other resonances which have small contributions.

3. Extraction of the $\overline{K^*}$ channels

In order to correct for the appreciable background under each contributing quasi-two-body process we have developed a method [12] which uses all four relevant independent variables describing the three-particle final state from an unpolarised target. The coefficients of the Legendre polynomial expansions of the differential cross section and density matrix elements for all quasi-two-body processes included are extracted simultaneously. Interference effects between contributing processes have been neglected; the fact that the data are reasonably well fitted at all energies with an incoherent production model suggests that such effects are small.

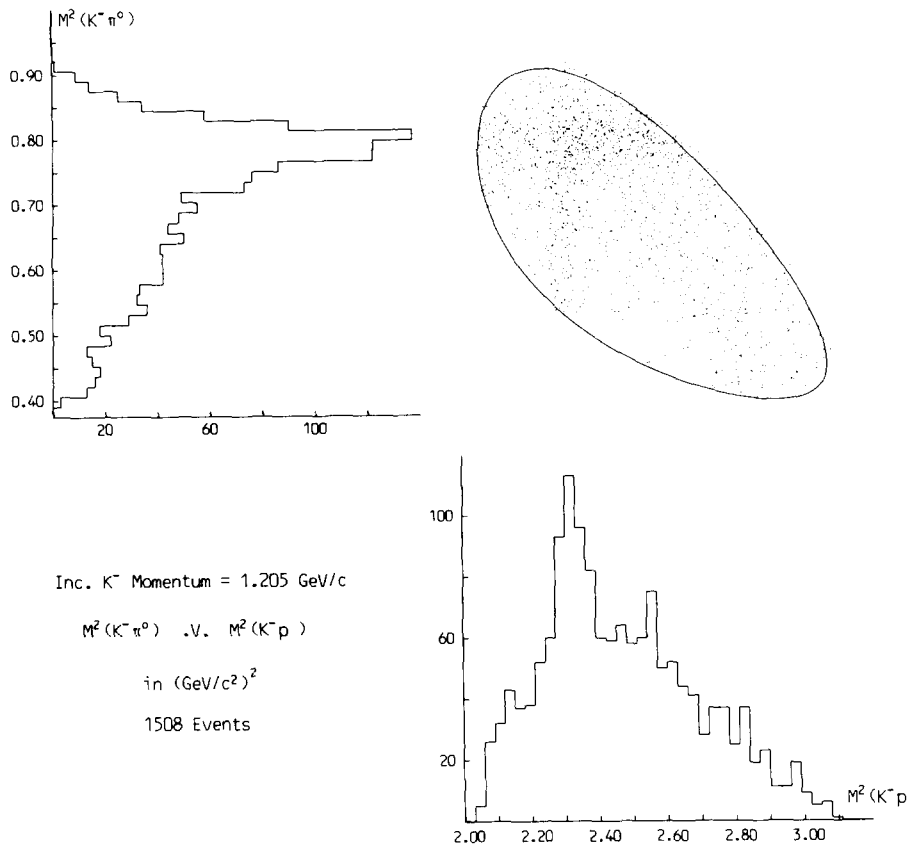

Fig. 2c.

The probability distribution W for reaction (2) decaying to KπN is given by

$$W(\cos\theta^*, \theta, \phi, M^2) = \frac{3}{4\pi} B(M^2) \frac{1}{\sigma} \frac{\mathrm{d}\sigma}{\mathrm{d}\cos\theta^*} [\tfrac{1}{2}(1 - \rho_{00}) + \tfrac{1}{2}(3\rho_{00} - 1)\cos^2\theta$$

$$- \rho_{1-1} \sin^2\theta \cos 2\phi - \sqrt{2}\,\mathrm{Re}\,\rho_{10} \sin 2\theta \cos\phi] \,, \qquad (5)$$

where θ^* is the c.m. production angle of the K*, θ and ϕ are the decay angles in the helicity frame of the K*, M^2 is the invariant Kπ mass-squared, $B(M^2)$ is the relativistic Breit-Wigner form (normalised to unity over the available phase space) with energy independent width for the K* and the expression in the square brackets describes the K* decay distribution in terms of density matrix elements ρ_{00}, ρ_{1-1} and Re ρ_{10}, which are themselves functions of the production angle. Following the formalism set out by Deen [13], the differential cross sections and density matrix elements are

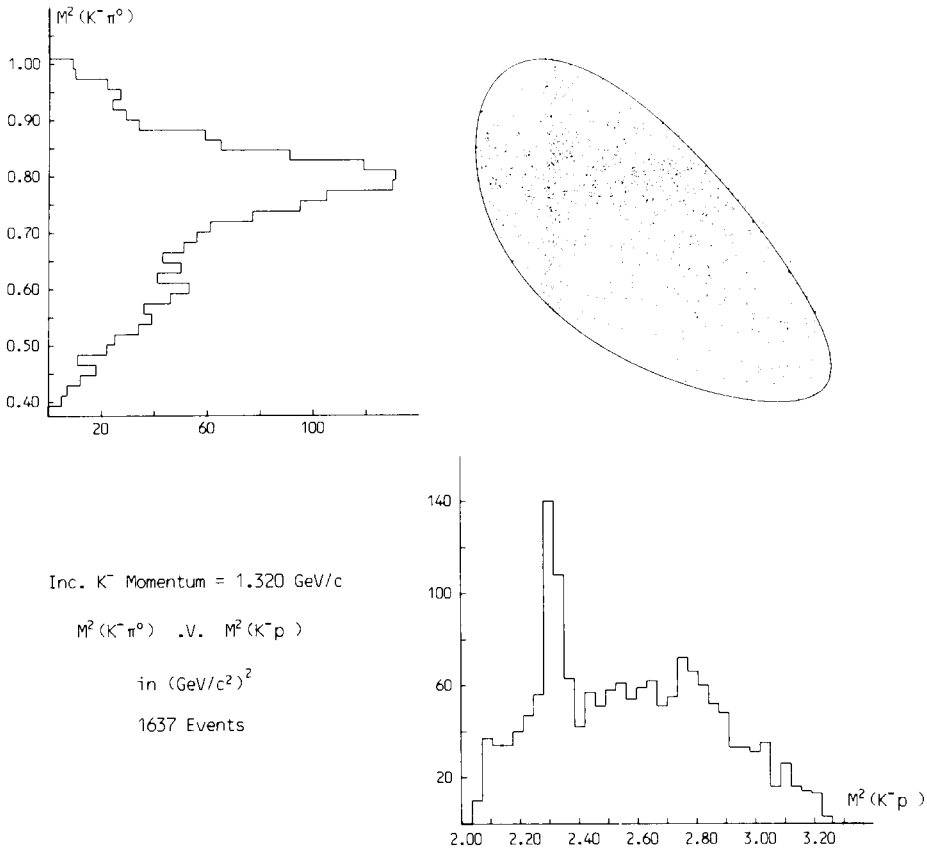

Fig. 2d.

expanded in Legendre polynomial series

$$\frac{d\sigma}{d\cos\theta^*} = 2\pi\lambda^2 \sum_l A_l P_l^0(\cos\theta^*) ,$$

$$\rho_{00}\frac{d\sigma}{d\cos\theta^*} = 2\pi\lambda^2 \sum_l B_l P_l^0(\cos\theta^*) , \tag{6}$$

$$\mathrm{Re}\,\rho_{10}\frac{d\sigma}{d\cos\theta^*} = 2\pi\lambda^2 \sum_l C_l P_l^1(\cos\theta^*) ,$$

$$\rho_{1-1}\frac{d\sigma}{d\cos\theta^*} = 2\pi\lambda^2 \sum_l D_l P_l^2(\cos\theta^*) .$$

Similar expressions are written for the other contributing quasi-two-body processes.

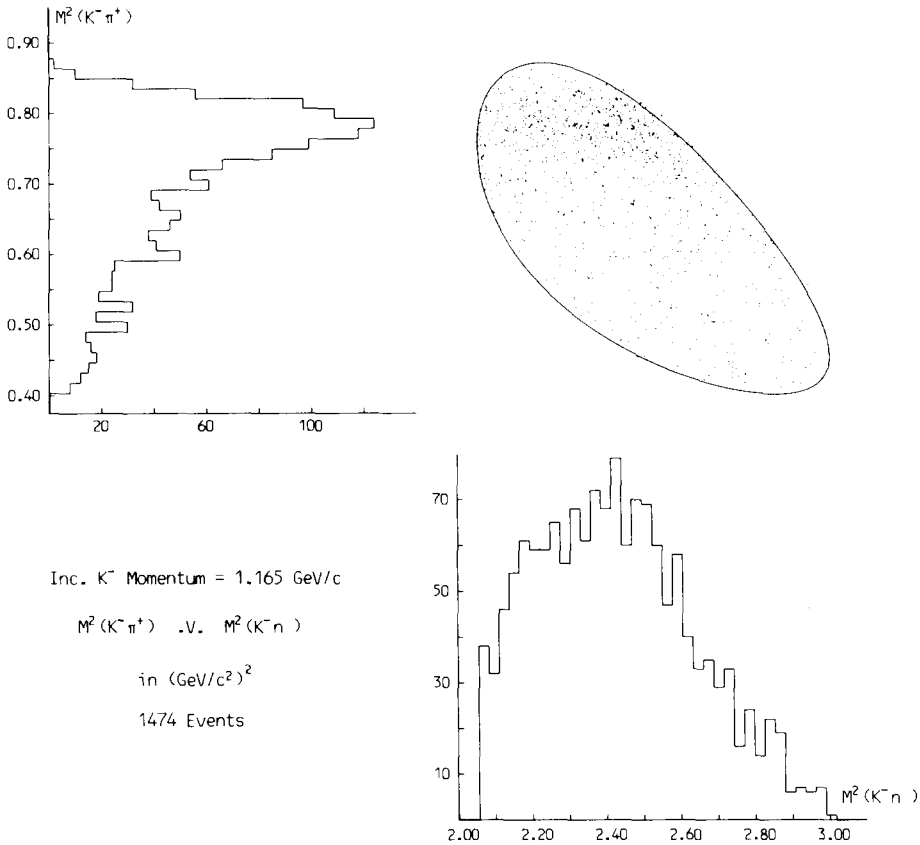

Fig. 2e.

The maximum order of expansion found necessary was $l = 7$. To improve the quality of the fit to the high $\bar{K}N$ mass region, production of the $\frac{3}{2}^-$ $\Lambda(1690)$ and $\frac{5}{2}^-\Sigma(1775)$ was included with simplified decay distributions. Finally, 3-particle Lorentz invariant phase space (LIPS) is included in each of the three reactions as incoherent background to contributing quasi-two-body processes mentioned.

The reliability of the expansion coefficients extracted for the K^* channel is confirmed by the fact that the two independent sets of coefficients obtained for the $K^{*-}(890)p$ channel from the $K^-p\pi^0$ and $\bar{K}^0p\pi^-$ final states are found to be consistent in spite of the rather different sets of contributing quasi-two-body processes involved. This fact indicates that the extraction procedure used is justified and therefore the use of a more complicated analysis is not warranted. The weighted means of these two sets were used as the final coefficients for the $K^{*-}p$ channel. Moreover the ratio $R = (pK^{*-} \to p\bar{K}^0\pi^-)/(pK^{*-} \to pK^-\pi^0)$ is found to be consistent with the expected value of 2.0 at each incident momentum and the overall mean is 1.97 ± 0.04.

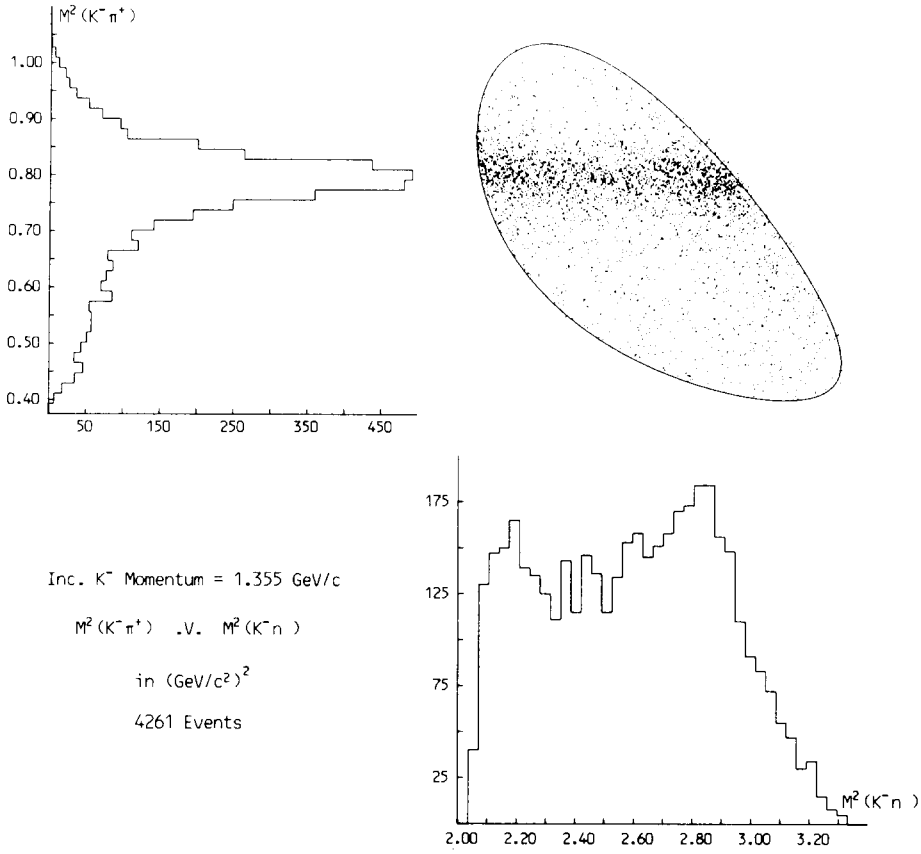
M² (K⁻π⁺)
1.00
0.90
0.80
0.70
0.60
0.50
0.40
50
150
250
350
450
Inc. K⁻ Momentum = 1.355 GeV/c
M² (K⁻π⁺) .V. M² (K⁻n)
in (GeV/c²)²
4261 Events
175
125
75
25
M² (K⁻n)
2.00
2.20
2.40
2.60
2.80
3.00
3.20

Fig. 2f.

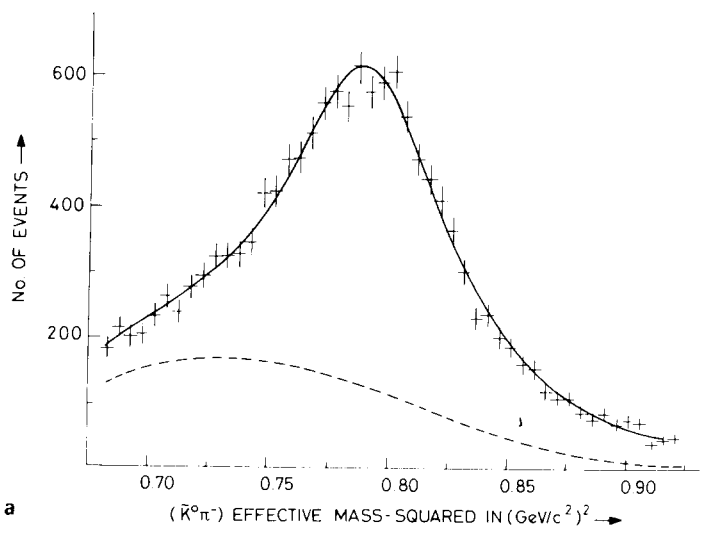
600
400
200
No OF EVENTS
0.70
0.75
0.80
0.85
0.90
(K̄°π⁻) EFFECTIVE MASS-SQUARED IN (GeV/c²)²
a

Fig. 3.

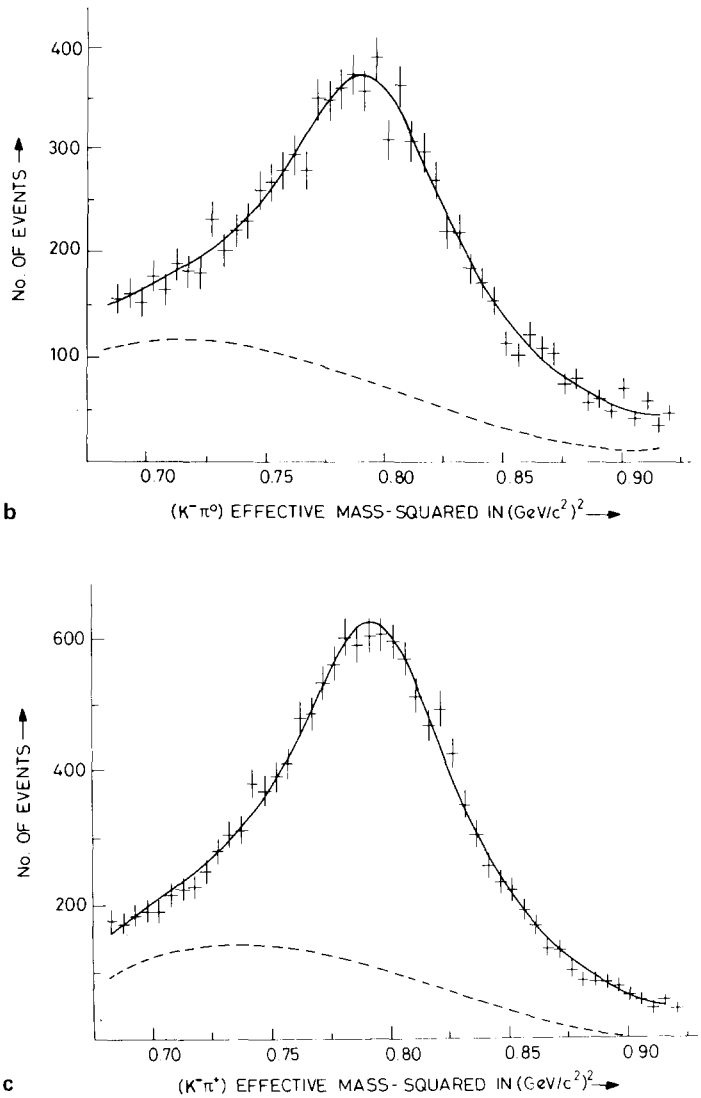

Fig. 3. $M^2(\bar{K}\pi)$ distributions in the region of the $K^*(890)$: (a) $\overline{K^0}\pi^-$; (b) $K^-\pi^0$; (c) $K^-\pi^+$. The curve is the result of the fit described in the text; the dashed line indicates the background under the resonance.

The relative cross sections for the various contributing processes to each of the three $\bar{K}\pi N$ final states are given in table 1. A complete set of coefficients for reactions (2a) and (2b) are given in tables 3 and 4. Some of the more significant coefficients are shown in fig. 4 along with those from the CRSS and the Birmingham

Table 3

Values of the experimental coefficients A_0, A_l/A_0, B_l/A_0, C_l/A_0 and D_l/A_0 for reaction (2a)

a

Momentum (GeV/c)		A0X10	A1/A0	A2/A0	A3/A0	A4/A0	A5/A0	A6/A0	A7/A0
0.960		0.102	0.906	1.208	0.915	1.149	-0.166	0.046	0.251
	+/-	0.011	0.266	0.367	0.426	0.471	0.536	0.600	0.658
1.005		0.111	0.634	0.462	0.961	1.207	0.146	-0.047	0.393
	+/-	0.017	0.221	0.343	0.368	0.476	0.496	0.523	0.546
1.045		0.250	0.633	0.230	0.655	0.578	-0.040	-0.205	0.434
	+/-	0.017	0.136	0.196	0.217	0.238	0.258	0.281	0.318
1.085		0.335	0.239	0.286	0.392	0.119	0.116	-0.210	-0.007
	+/-	0.030	0.126	0.163	0.183	0.213	0.240	0.256	0.276
1.125		0.556	0.090	0.121	0.125	-0.044	0.155	-0.172	-0.016
	+/-	0.030	0.099	0.126	0.146	0.171	0.187	0.200	0.213
1.165		0.758	0.343	0.356	0.661	0.188	0.155	0.116	-0.134
	+/-	0.032	0.084	0.109	0.128	0.145	0.161	0.173	0.184
1.205		0.949	0.650	0.661	0.736	0.456	0.227	0.189	0.137
	+/-	0.038	0.079	0.106	0.126	0.145	0.161	0.173	0.188
1.245		1.325	0.554	0.734	0.677	0.317	0.006	0.112	0.073
	+/-	0.043	0.065	0.081	0.097	0.110	0.121	0.129	0.138
1.285		1.489	0.708	0.971	0.754	0.324	-0.002	-0.134	0.047
	+/-	0.046	0.060	0.077	0.091	0.104	0.115	0.124	0.133
1.3[illegible]		1.699	0.834	1.073	0.708	0.014	-0.226	-0.247	-0.218
	+/-	0.056	0.063	0.076	0.092	0.109	0.119	0.127	0.137
1.3[illegible]		[illegible]	0.878	1.028	0.45[illegible]	-0.050	-0.285	-0.147	-0.050
	+/-	[illegible]	0.057	[illegible]	0.084	0.099	0.110	0.120	0.129

b

Momentum (GeV/c)		B1/A0	B2/A0	B3/A0	B4/A0	B4/A0	B5/A0	B6/A0	B7/A0
0.960		[illegible]	1.0[illegible]	1.126	[illegible]	0.257	0.183	0.225	0.377
	+/-	1.121	0.316	0.442	0.510	0.586	0.676	0.765	0.821
1.005		1.068	[illegible]	-0.003	0.646	0.520	-0.358	-0.704	0.410
	+/-	0.121	[illegible]	[illegible]	0.317	0.445	0.459	0.474	0.506
1.045		[illegible]	0.567	0.001	0.224	0.651	0.047	-0.284	0.173
	+/-	[illegible]	0.146	0.221	0.239	0.2[illegible]	0.287	0.304	0.340
1.085		0.555	0.338	0.320	0.216	0.667	-0.139	0.005	-0.467
	+/-	0.064	0.136	0.189	0.205	0.236	0.27[illegible]	0.284	0.306
1.125		0.78[illegible]	0.15[illegible]	-0.062	0.217	0.563	0.313	-0.269	-0.020
	+/-	0.047	0.083	0.124	0.130	0.153	0.164	0.185	0.197
1.165		0.423	0.13[illegible]	0.126	0.709	0.652	0.276	0.192	-0.072
	+/-	[illegible]	0.076	0.111	0.125	0.134	0.152	0.165	0.176
1.205		0.465	0.222	0.241	0.811	0.784	-0.023	0.052	0.172
	+/-	0.036	0.07[illegible]	[illegible]	0.123	0.138	0.156	0.169	0.183
1.245		[illegible].491	0.218	0.187	0.399	0.699	-0.070	0.191	0.081
	+/-	[illegible]	0.059	0.085	0.098	0.101	0.118	0.124	0.134
1.285		[illegible]	0.426	0.504	0.479	0.531	-0.026	-0.079	-0.093
	+/-	[illegible]	0.060	0.082	0.092	0.102	0.113	0.123	0.133
1.3[illegible]		[illegible]	[illegible]	0.569	[illegible]	0.150	-0.134	-0.157	[illegible]
	+/-	[illegible]	0.064	0.081	0.093	0.108	0.118	0.126	0.137
1.3[illegible]		[illegible]	[illegible]	0.588	0.455	0.350	-0.118	0.244	0.135
	+/-	[illegible]	[illegible]	[illegible]	0.093	0.104	0.116	0.125	0.133

Table 3 (continued)

c

Momentum (GeV/c)		$\langle Y_0^0 \rangle$	$\langle Y_1^0 \rangle$	$\langle Y_1^1 \rangle$	$\langle Y_2^0 \rangle$	$\langle Y_2^1 \rangle$	$\langle Y_2^2 \rangle$	$\langle Y_3^0 \rangle$	$\langle Y_3^1 \rangle$
0.960	−	0.0	0.032	−0.088	−0.042	−0.044	−0.079	−0.006	0.027
	+−	0.0	0.048	0.047	0.045	0.041	0.038	0.034	0.034
1.005	−	0.0	0.028	−0.083	0.061	0.061	0.064	0.005	0.011
	+−	0.0	0.043	0.044	0.048	0.045	0.043	0.038	0.039
1.045	−	0.0	0.108	0.028	0.058	0.055	0.071	0.019	0.047
	+−	0.0	0.046	0.044	0.047	0.039	0.037	0.026	0.031
1.085	−	0.0	0.100	−0.107	0.075	0.070	0.063	−0.018	0.012
	+−	0.0	0.047	0.043	0.052	0.045	0.041	0.029	0.028
1.125	−	0.0	0.082	−0.038	0.060	0.107	−0.026	0.030	−0.030
	+−	0.0	0.035	0.035	0.037	0.028	0.028	0.016	0.024
1.165	−	0.0	0.026	0.002	0.008	0.126	0.022	0.026	0.022
	+−	0.0	0.027	0.031	0.027	0.025	0.025	0.014	0.023
1.205	−	0.0	0.047	−0.044	0.047	0.088	0.005	0.013	0.026
	+−	0.0	0.024	0.019	0.026	0.025	0.024	0.013	0.022
1.245	−	0.0	−0.006	−0.023	0.017	0.067	−0.006	0.006	−0.006
	+−	0.0	0.018	0.015	0.018	0.017	0.017	0.010	0.019
1.285	−	0.0	0.086	0.014	0.056	0.083	−0.001	0.016	−0.013
	+−	0.0	0.026	0.024	0.027	0.027	0.027	0.011	0.019
1.325	−	0.0	0.075	0.014	0.042	0.055	−0.004	0.004	0.005
	+−	0.0	0.025	0.018	0.024	0.022	0.021	0.010	0.018
1.455	−	0.0	0.061	0.015	0.059	0.065	0.026	0.004	0.007
	+−	0.0	0.026	0.015	0.017	0.017	0.017	0.009	0.014

d

Momentum (GeV/c)		$\langle Y_0^0 \rangle$	$\langle Y_1^0 \rangle$	$\langle Y_1^1 \rangle$	$\langle Y_2^0 \rangle$	$\langle Y_2^1 \rangle$	$\langle Y_2^2 \rangle$	$\langle Y_3^0 \rangle$	$\langle Y_3^1 \rangle$
[illegible]	−	0.0	0.0	[illegible]	[illegible]	−0.075	0.034	0.027	0.007
	+−	0.0	0.0	0.025	0.023	0.020	0.021	0.004	0.012
[illegible]	−	0.0	0.0	[illegible]	−0.031	−0.031	0.009	0.010	0.007
	+−	0.0	0.0	0.017	0.015	0.014	0.009	0.008	0.007
[illegible]	−	0.0	0.0	−0.035	−0.004	−0.020	−0.012	−0.003	−0.006
	+−	0.0	0.0	0.014	0.013	0.009	0.006	0.003	0.004
[illegible]	−	0.0	0.0	−0.023	0.026	−0.010	0.001	0.001	0.002
	+−	0.0	0.0	0.011	0.011	0.008	0.006	0.004	0.004
[illegible]	−	0.0	0.0	−0.025	0.009	−0.013	−0.003	−0.002	0.003
	+−	0.0	0.0	0.015	0.009	0.008	0.004	0.003	0.005
[illegible]	−	0.0	0.0	−0.047	−0.009	−0.027	−0.008	−0.001	−0.002
	+−	0.0	0.0	0.018	0.015	0.015	0.009	0.003	0.007
[illegible]	−	0.0	0.0	−0.031	−0.013	−0.017	0.004	−0.002	−0.004
	+−	0.0	0.0	0.021	0.017	0.015	0.010	0.003	0.007
[illegible]	−	0.0	0.0	−0.045	−0.018	−0.021	0.0	0.002	−0.000
	+−	0.0	0.0	0.024	0.020	0.016	0.013	0.002	0.007
[illegible]	−	0.0	0.0	−0.033	−0.008	−0.014	−0.003	−0.002	−0.001
	+−	0.0	0.0	0.018	0.015	0.014	0.013	0.002	0.006
[illegible]	−	0.0	0.0	−0.047	−0.017	−0.032	−0.005	−0.005	−0.001
	+−	0.0	0.0	0.018	0.017	0.016	0.014	0.003	0.007
[illegible]	−	0.0	0.0	−0.043	−0.025	−0.035	−0.004	−0.004	−0.000
	+−	0.0	0.0	0.018	0.017	0.016	0.015	0.003	0.007

Table 4
Values of the experimental coefficients A_0, A_1/A_0, B_1/A_0, C_1/A_0 and D_1/A_0 for reaction (2b)

a

Momentum (GeV/c)		A0(*10)	A1/A0	A2/A0	A3/A0	A4/A0	A5/A0	A6/A0	A7/A0
0.960		0.094	0.655	1.015	1.272	0.773	1.143	0.841	0.787
	+/-	0.009	0.223	0.397	0.385	0.430	0.461	0.476	0.517
1.005		0.152	0.627	-0.019	0.698	0.619	-0.161	-0.151	0.226
	+/-	0.013	0.152	0.231	0.251	0.286	0.337	0.342	0.368
1.045		0.281	0.447	-0.100	0.278	-0.035	-0.087	-0.112	0.370
	+/-	0.014	0.096	0.128	0.150	0.187	0.199	0.223	0.231
1.085		0.537	0.239	-0.019	0.077	-0.147	-0.179	0.402	0.056
	+/-	0.034	0.085	0.109	0.138	0.152	0.164	0.180	0.195
1.125		1.015	0.047	-0.122	0.332	0.137	-0.093	0.019	-0.071
	+/-	0.034	0.064	0.086	0.101	0.116	0.127	0.141	0.152
1.165		1.241	-0.047	-0.167	0.068	-0.034	0.222	-0.135	0.012
	+/-	0.036	0.054	0.070	0.082	0.092	0.101	0.110	0.121
1.205		1.341	-0.051	-0.084	0.241	-0.076	0.054	0.137	0.027
	+/-	0.038	0.055	0.068	0.083	0.094	0.105	0.112	0.121
1.245		1.399	0.025	0.147	0.197	0.031	-0.049	0.035	0.064
	+/-	0.035	0.049	0.064	0.076	0.086	0.094	0.102	0.110
1.285		1.488	0.106	0.390	0.371	-0.116	-0.190	0.046	-0.072
	+/-	0.036	0.051	0.063	0.075	0.086	0.096	0.104	0.110
1.328		1.372	0.152	0.518	0.376	-0.074	0.036	-0.119	-0.103
	+/-	0.037	0.059	0.072	0.085	0.096	0.107	0.117	0.123
1.355		1.569	0.221	0.626	0.353	-0.209	-0.146	-0.008	0.053
	+/-	0.035	0.047	0.055	0.067	0.077	0.085	0.093	0.099

b

Momentum (GeV/c)		B0/A0	B1/A0	B2/A0	B3/A0	B4/A0	B5/A0	B6/A0	B7/A0
0.960		0.540	0.147	0.483	0.938	0.585	1.288	0.850	0.895
	+/-	0.097	0.234	0.335	0.426	0.507	0.571	0.612	0.640
1.005		0.565	0.076	-0.413	0.908	0.869	-0.233	0.256	0.732
	+/-	0.093	0.149	0.261	0.287	0.324	0.376	0.358	0.404
1.045		0.484	0.009	-0.135	0.543	0.271	0.107	0.080	0.123
	+/-	0.056	0.098	0.142	0.164	0.206	0.211	0.240	0.242
1.085		0.467	0.001	-0.064	0.345	0.075	-0.364	0.188	0.056
	+/-	0.045	0.084	0.109	0.137	0.149	0.157	0.178	0.192
1.125		0.492	-0.113	-0.184	0.377	0.464	0.066	0.102	0.059
	+/-	0.034	0.061	0.090	0.104	0.117	0.131	0.144	0.154
1.165		0.451	-0.151	-0.112	0.201	0.256	0.075	0.035	-0.002
	+/-	0.028	0.051	0.071	0.082	0.089	0.096	0.105	0.115
1.205		0.374	-0.110	-0.178	0.060	0.147	-0.067	0.035	-0.023
	+/-	0.026	0.044	0.061	0.072	0.083	0.093	0.098	0.105
1.245		0.443	-0.027	0.001	0.225	0.308	-0.028	0.074	0.021
	+/-	0.023	0.046	0.064	0.075	0.085	0.096	0.103	0.109
1.285		0.468	0.072	0.047	0.153	0.224	-0.260	-0.155	-0.039
	+/-	0.024	0.047	0.063	0.072	0.082	0.091	0.098	0.105
1.328		0.455	0.113	0.131	0.168	0.151	-0.138	-0.014	-0.122
	+/-	0.027	0.055	0.072	0.083	0.091	0.101	0.111	0.117
1.355		0.480	0.100	0.212	0.231	0.132	-0.258	-0.018	0.052
	+/-	0.021	0.045	0.057	0.066	0.075	0.082	0.091	0.097

Table 4 (continued)

c

Momentum (GeV/c)		C0/A0	C1/A0	C2/A0	C3/A0	C4/A0	C5/A0	C6/A0	C7/A0
0.960		0.0	0.027	0.068	0.005	-0.039	-0.044	-0.001	-0.027
	+/-	0.0	0.051	0.043	0.033	0.031	0.031	0.032	0.028
1.005		0.0	0.002	0.106	0.098	-0.002	0.005	0.027	-0.035
	+/-	0.0	0.061	0.039	0.037	0.030	0.028	0.026	0.025
1.045		0.0	0.008	-0.013	0.047	0.056	-0.040	0.009	0.025
	+/-	0.0	0.038	0.027	0.022	0.017	0.017	0.016	0.015
1.085		0.0	-0.040	-0.016	0.039	0.074	0.010	-0.031	0.028
	+/-	0.0	0.031	0.023	0.018	0.016	0.015	0.014	0.012
1.125		0.0	-0.009	-0.023	0.023	0.027	0.008	0.012	0.005
	+/-	0.0	0.024	0.017	0.014	0.012	0.011	0.010	0.010
1.165		0.0	-0.055	-0.033	0.024	0.052	0.012	0.000	-0.013
	+/-	0.0	0.020	0.015	0.012	0.011	0.010	0.009	0.008
1.205		0.0	-0.045	-0.026	-0.010	0.042	0.000	-0.011	0.006
	+/-	0.0	0.019	0.014	0.011	0.010	0.009	0.008	0.007
1.245		0.0	-0.046	-0.042	-0.011	0.054	-0.011	0.009	-0.001
	+/-	0.0	0.016	0.012	0.010	0.009	0.008	0.008	0.007
1.285		0.0	-0.029	-0.031	-0.025	0.047	-0.018	-0.002	-0.016
	+/-	0.0	0.015	0.012	0.010	0.009	0.008	0.008	0.007
1.320		0.0	0.013	-0.033	-0.025	0.041	-0.025	-0.007	-0.002
	+/-	0.0	0.017	0.014	0.012	0.010	0.009	0.009	0.008
1.355		0.0	-0.015	-0.028	-0.018	0.033	-0.005	0.016	0.002
	+/-	0.0	0.013	0.011	0.010	0.008	0.007	0.007	0.006

d

Momentum (GeV/c)		D0/A0	D1/A0	D2/A0	D3/A0	D4/A0	D5/A0	D6/A0	D7/A0
0.960		0.0	0.0	-0.024	0.014	0.001	0.001	0.014	0.005
	+/-	0.0	0.0	0.024	0.015	0.011	0.008	0.007	0.005
1.005		0.0	0.0	-0.026	-0.047	-0.021	-0.002	-0.007	-0.004
	+/-	0.0	0.0	0.029	0.014	0.010	0.007	0.005	0.004
1.045		0.0	0.0	-0.035	0.007	-0.005	0.003	0.007	-0.001
	+/-	0.0	0.0	0.014	0.009	0.007	0.004	0.005	0.003
1.085		0.0	0.0	-0.006	-0.012	-0.003	0.001	0.007	-0.002
	+/-	0.0	0.0	0.016	0.008	0.005	0.004	0.005	0.003
1.125		0.0	0.0	-0.044	0.002	-0.010	-0.005	-0.001	0.002
	+/-	0.0	0.0	0.013	0.006	0.004	0.003	0.002	0.002
1.165		0.0	0.0	-0.046	0.008	-0.008	0.003	0.001	-0.000
	+/-	0.0	0.0	0.011	0.005	0.004	0.003	0.002	0.002
1.205		0.0	0.0	-0.019	0.008	-0.014	0.001	0.002	0.000
	+/-	0.0	0.0	0.010	0.005	0.004	0.002	0.002	0.002
1.245		0.0	0.0	-0.020	0.023	-0.009	0.004	0.001	0.001
	+/-	0.0	0.0	0.009	0.005	0.003	0.002	0.002	0.001
1.285		0.0	0.0	-0.013	0.027	-0.005	0.002	0.001	-0.004
	+/-	0.0	0.0	0.008	0.005	0.003	0.002	0.002	0.001
1.320		0.0	0.0	-0.003	0.026	-0.007	0.002	-0.003	-0.002
	+/-	0.0	0.0	0.009	0.005	0.004	0.003	0.003	0.002
1.355		0.0	0.0	-0.021	0.027	-0.012	0.001	-0.002	-0.001
	+/-	0.0	0.0	0.007	0.004	0.003	0.002	0.002	0.001

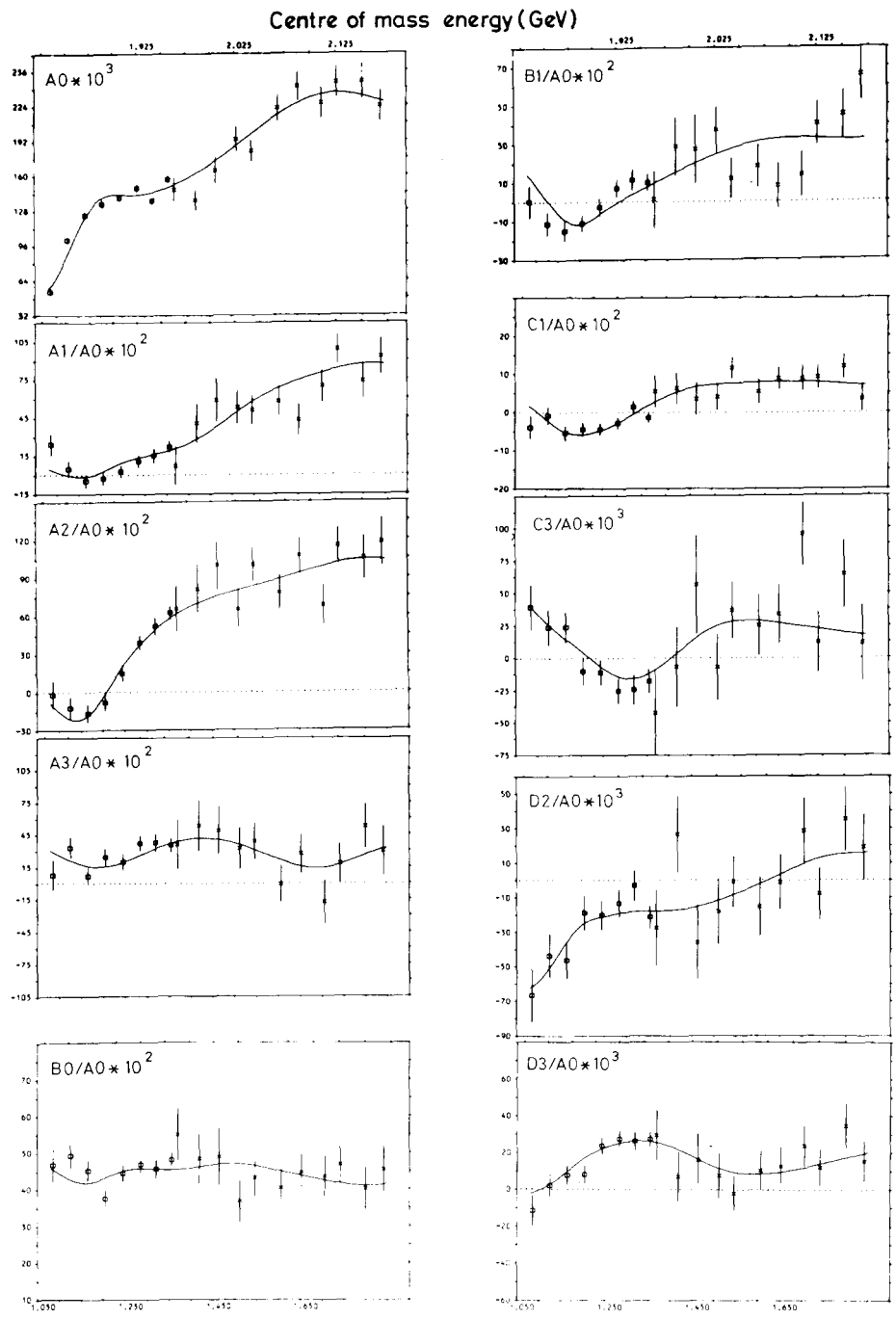

Fig. 4. A selection of Legendre polynomial coefficients as a function of c.m. energy and incident momenta: (a) for $K^-p \to K^{*-}p$; (b) for $K^-p \to K^{*0}n$; (c) for $K^-n \to K^{*-}n$. The curves are the results of the partial-wave analysis. The data from the present experiment is shown by □, the CRSS data by × and the Birmingham data by ◇.

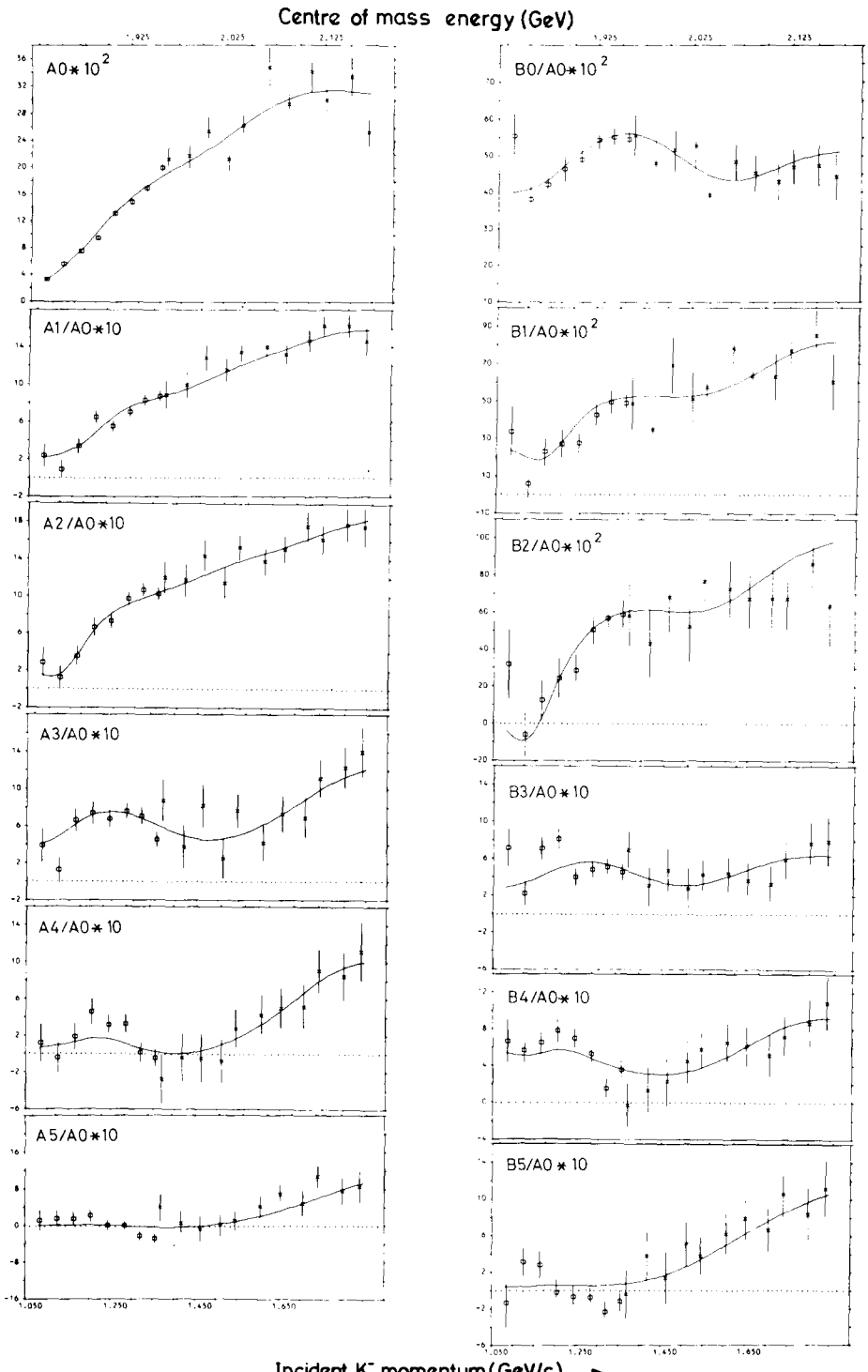

b

Fig. 4 (continued).

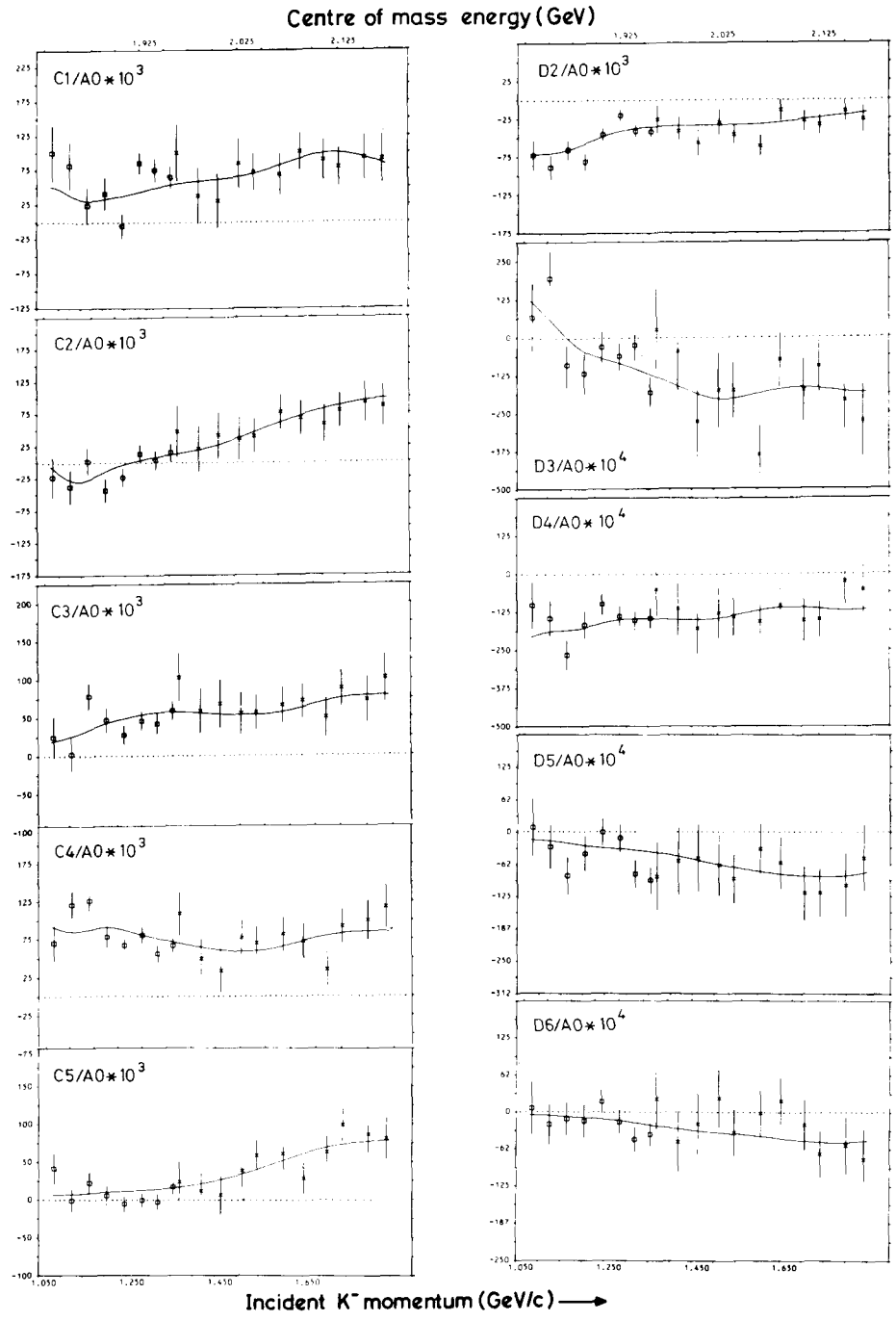

b

Fig. 4 (continued).

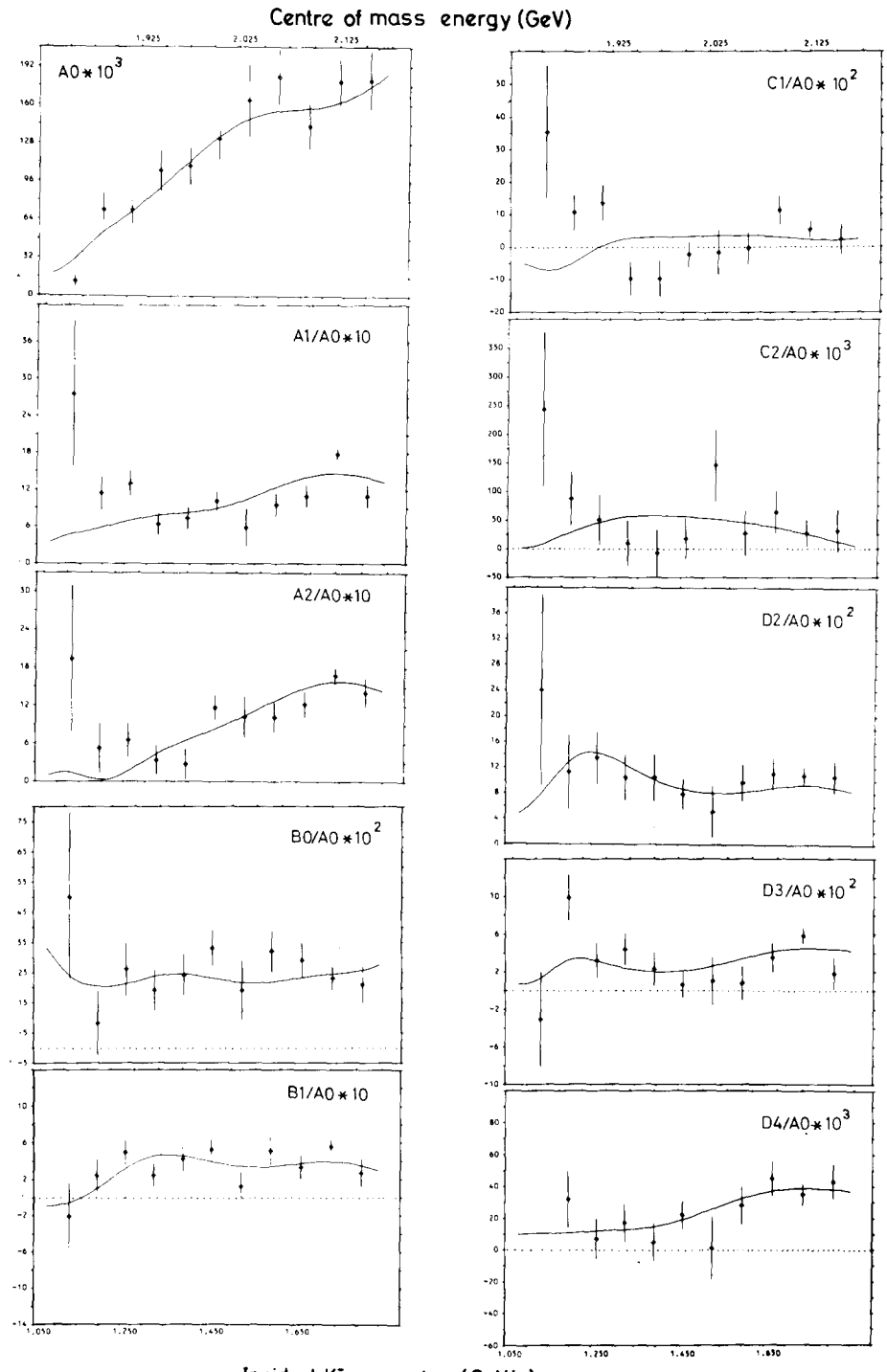

c

Fig. 4 (continued).

experiments. The three lowest momenta are below the threshold for the production of a $K\pi$ system with a mass equal to the K^* mass, and therefore the data used in the partial-wave analysis are those for momenta above 1.045 GeV/c.

4. Partial-wave analysis

An energy dependent partial-wave analysis of the reaction $\bar{K}N \to \bar{K}^*N$ has been carried out between 1830 and 2170 MeV c.m. energy using a combination of data from the present experiment and those from two previous experiments [1,2]. The data used in the partial-wave analysis are listed in table 5.

4.1. The parametrisation

A partial-wave amplitude $T(I, L, L', 2J, 2S')$ where I is the isotopic spin, L and L' are the incoming and outgoing orbital angular momenta, J is the total angular momentum, and S' the spin of the K^*N system, is parametrised as

$$T = T_B + T_R \ , \tag{7}$$

where T_B is the background term and T_R is a sum of non-relativistic Breit-Wigner

Table 5
The data used in this analysis and the χ^2 contribution to the solution of each data set given as χ^2 per data point

Momentum Range (GeV/c)	c.m. Energy Range (MeV/c)	Experiment	No. of Momenta	Type of Data	No. of Data Points				χ^2/Data Point			
					$\bar{K}^{*0}n$	$K^{*-}p$	$K^{*-}n$	Total	$\bar{K}^{*0}n$	$K^{*-}p$	$K^{*-}n$	Total
1.085–1.355	1833–1957	This Expt.	8	$A_0, A_1/A_0$	64	64	-	128	1.26	1.32	-	1.29
				B_1/A_0	64	64	-	128	1.50	1.03	-	1.21
				C_1/A_0	56	56	-	112	1.41	1.15	-	1.28
				D_1/A_0	48	48	-	96	1.12	1.05	-	1.08
1.370–1.841	1964–2168	CRSS [1]	11	$A_0, A_1/A_0$	88	88	-	176	0.85	1.02	-	0.94
				B_1/A_0	88	88	-	276	0.55	1.19	-	0.87
				C_1/A_0	77	77	-	154	0.55	0.90	-	0.73
				D_1/A_0	66	66	-	132	0.64	0.94	-	0.79
1.132–1.810	1855–2155	Birmingham [2]	11	$A_0, A_1/A_0$	-	-	80	80	-	-	1.81	1.81
				B_1/A_0	-	-	80	80	-	-	1.36	1.36
				C_1/A_0	-	-	69	69	-	-	1.46	1.46
				D_1/A_0	-	-	58	58	-	-	0.89	0.89
1.085–1.841	1833–2168	All Expts.	30	$A_0, A_1/A_0$	152	152	80	384	1.02	1.15	1.81	1.25
				B_1/A_0	152	152	80	384	0.91	1.12	1.36	1.09
				C_1/A_0	133	133	69	335	0.91	1.00	1.56	1.06
				D_1/A_0	114	114	58	286	0.84	0.99	0.89	0.90
				All	551	551	287	1,389	0.93	1.07	1.41	1.08

resonances of the form

$$\frac{t}{\epsilon - i} e^{i\phi} , \tag{8}$$

where t is the resonance amplitude and $\epsilon = 2(E_R - E)/\Gamma(E)$. The energy dependent width, Γ, is of the form

$$\Gamma(E) = \Gamma(E_R) \frac{k v_l(kr)}{k_R v_l(k_R r)} , \tag{9}$$

where v_l is the Blatt and Weisskopf angular momentum barrier [14] for the incoming orbital angular momentum l. The radius of interaction, r, is taken to be 1 fm. In these formulae E is the c.m. energy and E_R and k_R are the values of E and k at the resonance energy and $t = \sqrt{xx'} = \sqrt{\Gamma_e \Gamma_i / \Gamma^2}$, Γ_e and Γ_i being the partial widths of the elastic and the $\overline{K}^*N$ channels respectively. The elastic partial width Γ_e has the same energy dependence as the total width. For Γ_i, k and k_R in the formula correspond to the c.m. momenta of the outgoing particles and l refers to the outgoing orbital angular momentum. Because of the finite width of the K^*, for both the resonant and background amplitudes the function kv_l is replaced by its value weighted by the K^* lineshape and averaged over the range $M_{K^*} - 2\Gamma_{K^*}$ to $M_{K^*} + 2\Gamma_{K^*}$. To ensure that the effects of high-spin resonances below threshold are negligible at energies greater than two widths above the mass of the resonance, the amplitude used is of the form

$$t = \sqrt{xx'} \exp\left[-\left(\frac{E - E_R}{\Gamma}\right)^4\right] . \tag{10}$$

The background term has the form

$$T_B = \sqrt{B_l B_{l'}} R(E) e^{i\theta(E)} , \tag{11}$$

where

$$R(E) = \sum_{m=0}^{M} a_m P_m(E') , \qquad \theta(E) = \sum_{n=0}^{N} b_n P_n(E') ,$$

and

$$E' = \frac{2E - E_{max} - E_{min}}{E_{max} - E_{min}} ,$$

such that E' equals + 1 and −1 at energies E_{max} and E_{min} just above the upper end below the lower end of the energy range fitted, and P_L are Legendre polynomials. The background parameters a_m and b_n are determined by fitting.

The angular momentum barrier factor B_l has the form

$$B_l = \frac{k}{k_{\max}} \frac{E_{\max}}{E} \frac{v_l(kr)}{v_l(k_{\max} r)} . \tag{12}$$

The various expansion coefficients of eq. (6) may be related to the partial-wave amplitudes by

$$\eta_l = \sum_{N_1} \sum_{N_2} x_{N_1}^{N_2} \operatorname{Re}(T_{N_1} T_{N_2}^*) , \tag{13}$$

where η_l is any of the coefficients $A_l - D_l$, and the x are the quasi-two-body equivalents of the Tripp coefficients [15] and N_i stands for the quantum numbers $I_i L_i L_i' J_i S_i'$.

4.2. The partial-wave solution

Since the highest order for which the Legendre polynomial coefficients have significant values is 7, it is necessary to allow for incident partial waves up to and including G7. In general each incident partial wave couples to more than one outgoing partial wave. With both $I = 0$ and $I = 1$ amplitudes present this gives a total of 44 partial wave amplitudes to determine. A general approach with variable backgrounds allowed in all waves leads to an unreasonably large number of free parameters. We have, therefore, attempted to develop a solution with a minimum number of free parameters including background amplitudes as required.

Hereafter, for a given incident partial wave (LIJ), the outgoing waves coupled to it are referred to by the quantum numbers ($L'S'$). Within the energy range 1830–2170 MeV there are two established $I = 1$ states, F15(1920), F17(2040), and two $I = 0$ states, P03(1900), G07(2110). Also, the established resonances D15(1775), D05(1825) and F05(1822) which are below or near threshold might couple to this channel.

An initial basic solution was developed with these resonances and no background amplitudes in any of the partial waves. The masses and widths were fixed to the values found in the partial-wave analysis of two-body channels [16]. The resonant amplitudes were constrained to be purely imaginary at the resonance mass. This solution gave a χ^2 of 8707 for 1368 degrees of freedom.

At this stage the less well established resonances S11(1955), D13(1920), S01(1825), P01(1853) and F05(2100) [16] were added. Again the masses and widths were fixed and the amplitudes constrained to be purely imaginary at the resonance masses. After refitting, this solution gave a χ^2 of 4438 for 1356 degrees of freedom. To improve the fit further, background amplitudes were then introduced. This was done iteratively. In the first iteration two parameter backgrounds ($N = M = 0$ see eq. (11)) were tried in each wave in turn and retained for that wave which gave the largest improvement in χ^2. The second iteration permitted either a second wave to carry $N = M = 0$

background or an increase in order of the background already found. This process of iteration was continued until there was no further significant improvement in χ^2.

For each incident partial wave, background amplitudes were found necessary in at least one outgoing wave, with the exception of the D05, F15 and F17 waves. This solution gave a χ^2 of 1564 for 1296 degrees of freedom with a total of 93 parameters. A significant number of the outgoing partial waves required background amplitudes with four or more parameters. Presence of any new resonant structures in any of these waves was investigated along with the significance of the 'less well established' resonances. Where the resonant amplitudes were large, attempts were made to see if the analysis of this channel preferred significantly different values for the mass and width of a given resonance from those given by the 2-body channels. A wave-by-wave description is given below.

4.2.1. The I = 0 waves

S01. The S01(1825) has large couplings to both S1 and D3 outgoing waves. Being just below threshold its mass was not allowed to vary, but the width when freed remained compatible with the value obtained in the two-body channels [16]. The D3 wave has a four-parameter background amplitude which describes an anti-clockwise loop. This could be replaced by a resonance at 2030 MeV with a width of 125 MeV and a two-parameter background, giving an improvement of ~15 in the χ^2.

P01. With the mass and width of the P01(1853) fixed, the P3 outgoing wave has an amplitude close to the unitarity limit value of 0.5 superimposed on a large anti-clockwise background. The fact that the total amplitude in this wave is still well within the unitarity limit, indicates that there is a large amount of cancellation between the resonant and the background amplitudes. This unsatisfactory behaviour is avoided when the width of the resonance is constrained to be narrow. The resonant amplitude then has a more reasonable magnitude. This channel, therefore, suggests that the width of the P01(1853) might be considerably narrower than is indicated by the two-body analyses [16].

P03. The established *P03*(1900) couples significantly only to the P1 outgoing wave where there is also a large slowly varying background amplitude.

D03. This wave requires a large two-parameter background amplitude in the D1 outgoing wave. No amplitudes are required in the other two outgoing waves.

D05. The established resonance D05(1825) which is just below threshold is found to have essentially zero coupling to this channel (<0.02 in all three outgoing waves) and no background amplitudes are required.

F05. Similarly the coupling to this channel of the established F05(1822) which is also just below threshold is essentially zero. The less well established F05(2100) shows a significant coupling to the F1 outgoing wave. Allowing the mass and width of this resonance to vary gives values of 2125 and 165 MeV respectively. Only the P3 outgoing wave has a significant background amplitude.

F07. There is a large two-parameter background amplitude in the F1 outgoing wave which is the only significant one.

G07. The established G07(2110) shows a large coupling in the D3 outgoing wave. The parameters of this resonance, when allowed to vary, do not change significantly from the initial values. There is a small background in the G3 outgoing wave.

4.2.2. The I = 1 waves

S11. The S11(1955) resonance has significant amplitudes in both the S1 and D3 outgoing waves superimposed on large four-parameter backgrounds. When allowed to vary, the mass and width of the resonance do not change appreciably from the initial values. In the D3 wave the background amplitude describes a tight anti-clockwise loop near the top end of the energy range covered. It was not however possible to replace this structure with a resonance having stable parameters.

P11. The P1 outgoing wave requires no amplitude, whereas the P3 wave has a large six-parameter background that is highly suggestive of a resonance. When a resonance is introduced at 1870 MeV with a width of 80 MeV, a two-parameter background is found to be sufficient and the quality of the fit is slightly improved. Without the resonance and only a two-parameter background in the P3 wave, the overall χ^2 is 60 units worse. This resonance could well be the state seen in a multi-channel analysis by Lea, Martin, Moorhouse and Oades [17] with an elasticity of 0.3. It has also been observed in an energy independent partial-wave analysis of the $\bar{K}N$ channel by Hansen, Moss and Oades [18].

P13. Only two parameter background amplitudes are found necessary in the P1 and P3 outgoing waves.

D13. The S3 outgoing wave has a significant four-parameter background amplitude describing an anti-clockwise loop which is essentially in the opposite quadrant to the large resonant amplitude for the D13(1920) resonance. There is, therefore, considerable cancellation between the two amplitudes. When the mass and width of the D13(1920) are allowed to vary, the resonance becomes considerably narrower and there is little energy variation in the background amplitude and an equally good fit is obtained with only a two-parameter background. The narrow width is consistent with that determined in ref. [18].

D15. The established D15(1774) which is just below threshold has effectively no coupling to this channel. There is a large two-parameter background amplitude in the F1 outgoing wave and a slowly varying four-parameter background in the D3 wave.

F17. The solution requires no backgrounds under the small resonant amplitudes for the established F17(2040).

G17. Small two-parameter background amplitudes are found necessary in the D3 and G3 outgoing waves.

4.2.3. The final solution

With new values for the widths of the P01(1853) and the D13(1920) and the replacement of higher order anticlockwise background amplitudes by new resonances

Table 6
Resonance amplitudes for $\bar{K}N \to \bar{K}^*(890)N$

Wave (L,2I)	Resonance parameters in MeV		(a) Elasticity	Outgoing wave (L'S')	$t_{\bar{K}^*(890)N}$	Branching Fraction to $\bar{K}^*N$
	M	Γ				
S01	(1825)	(230)	0.37 ± .05	S1	+0.17 ± .03	0.078
				D3	-0.13 ± .04	0.056
S01	2030 ± 30	125 ± 25	-	S1	+0.12 ± .03	-
				D3	+0.09 ± .03	
S11	(1955)	(170)	0.44 ± .05	S1	-0.10 ± .02	0.023
				D3	-0.07 ± .03	0.011
P01	(1853)	90 ± 20	0.21 ± .04	P1	+0.14 ± .03	0.093
				P3	+0.35 ± .06	0.583
P11	1870 ± 10	80 ± 10	0.30 ± .05 (b)	P1	+0.05 ± .03	0.008
				P3	+0.11 ± .03	0.040
P03	(1900)	(72)	0.18 ± .02	P1	+0.07 ± .03	0.027
				P3	<0.03	-
				F3	<0.03	-
D13	(1920)	170 ± 25	-	S3	-0.09 ± .02	-
				D1	<0.03	-
				D3	<0.03	-
F05	2125 ± 25	160 ± 30	0.07 ± .03	P3	<0.03	-
				F1	+0.17 ± .04	0.413
				F3	<0.03	-
F17	(2040)	(190)	0.24 ± .02	F1	-0.06 ± .03	0.015
				F3	+0.04 ± .03	0.007
				H3	<0.03	-
G07	(2110)	(250)	0.30 ± .03	D3	+0.21 ± .04	0.147
				G1	+0.04 ± .03	0.005
				G3	<0.03	-

(a) Values for the elasticity taken from Reference [16].

(b) Average value of the elasticities reported in PDG tables and in Reference [18].

Masses and widths in parentheses are from ref. [16].

in the S01 and P11 waves, the final solution has a χ^2 of 1506 for 1292 degrees of freedom. Apart from close to threshold, the general features of the data are well explained by this solution as can be seen from fig. 4. The resonance parameters obtained in the final fit are given in table 6. The partial-wave amplitudes at intervals of 10 MeV c.m. energy are presented in table 7, and the Argand diagrams for the active partial waves are shown in fig. 5.

Table 7
$\overline{K}N \to K^*(890)N$ partial-wave amplitudes give as real and imaginary parts at 10 MeV c.m. energy intervals

Ecm	1SS01		3SD01		1PP01		3PP01		1PP03		3PP03		3PF03	
1.83	0.12	0.10	0.01	-0.11	0.05	0.07	0.15	0.12	0.02	0.09	-0.02	0.02	-0.00	0.00
1.84	0.14	0.10	0.03	0.12	0.05	0.09	0.14	0.18	0.01	0.10	-0.02	0.02	-0.00	-0.00
1.85	0.16	0.10	0.04	0.13	0.03	0.12	0.11	0.24	0.01	0.11	-0.02	0.02	0.01	0.00
1.86	0.18	0.10	0.06	-0.14	0.01	0.14	0.06	0.29	0.01	0.13	-0.03	0.02	0.01	0.01
1.87	0.20	0.09	0.08	0.16	0.02	0.15	-0.01	0.31	0.01	0.15	-0.03	0.02	-0.01	0.01
1.88	0.22	0.09	0.11	-0.16	-0.05	0.14	-0.08	0.29	0.00	0.17	0.03	0.02	0.01	0.02
1.89	0.23	0.08	0.13	-0.17	0.07	0.13	-0.13	0.26	0.01	0.19	-0.03	0.01	-0.01	-0.02
1.90	0.24	0.07	0.16	-0.17	-0.09	0.11	-0.16	0.22	-0.04	0.20	-0.02	0.01	-0.00	-0.03
1.91	0.25	0.06	0.18	0.17	-0.09	0.09	-0.17	0.18	-0.06	0.21	0.02	0.01	0.01	0.03
1.92	-0.26	0.05	0.20	0.16	-0.10	0.08	-0.17	0.15	-0.08	0.20	0.01	0.02	0.02	-0.03
1.93	0.27	0.05	0.22	-0.15	-0.10	0.07	-0.16	0.13	-0.10	0.20	-0.01	0.03	0.02	-0.03
1.94	0.27	0.04	0.23	-0.14	-0.09	0.06	-0.16	0.11	-0.11	0.19	-0.01	0.03	0.02	-0.02
1.95	-0.27	0.03	0.25	-0.12	0.09	0.05	-0.15	0.09	-0.12	0.19	-0.01	0.04	0.03	-0.02
1.96	0.28	0.03	0.26	-0.10	-0.09	0.05	-0.14	0.08	-0.12	0.18	-0.01	0.04	0.03	-0.02
1.97	0.28	0.03	0.26	0.08	-0.09	0.04	-0.13	0.07	-0.13	0.18	-0.02	0.04	0.03	-0.01
1.98	0.28	0.03	0.27	-0.06	-0.08	0.04	-0.12	0.07	-0.14	0.18	-0.02	0.05	0.03	-0.01
1.99	0.28	0.03	0.26	-0.03	-0.08	0.03	-0.11	0.06	-0.14	0.17	-0.02	0.05	0.03	-0.01
2.00	0.29	0.04	0.26	-0.01	-0.08	0.03	-0.11	0.06	-0.15	0.17	-0.02	0.05	0.03	-0.01
2.01	0.30	0.04	0.24	0.02	0.08	0.03	-0.10	0.06	-0.16	0.17	-0.02	0.05	0.03	-0.01
2.02	0.31	0.04	0.23	0.04	-0.07	0.02	-0.10	0.06	-0.16	0.16	-0.02	0.06	0.03	-0.01
2.03	0.32	0.04	0.20	0.06	-0.07	0.02	-0.09	0.06	-0.17	0.16	-0.02	0.06	0.03	-0.01
2.04	0.34	0.03	0.18	0.08	-0.07	0.02	-0.09	0.06	-0.18	0.16	-0.03	0.06	0.03	-0.01
2.05	0.35	0.01	0.15	0.09	0.07	0.02	-0.09	0.06	-0.18	0.15	-0.03	0.06	0.03	-0.01
2.06	0.36	0.01	0.13	0.10	-0.06	0.02	-0.08	0.06	-0.19	0.15	-0.03	0.06	0.03	-0.01
2.07	0.37	0.02	0.10	0.10	-0.06	0.02	-0.08	0.06	-0.19	0.14	-0.03	0.06	0.03	-0.01
2.08	0.37	0.04	0.09	0.11	-0.06	0.01	-0.08	0.06	-0.20	0.14	-0.03	0.06	0.03	-0.01
2.09	0.37	-0.06	0.07	0.11	-0.06	0.01	-0.08	0.06	-0.21	0.13	-0.03	0.06	0.03	-0.01
2.10	0.36	0.07	0.05	0.11	-0.06	0.01	-0.08	0.06	-0.21	0.12	-0.03	0.07	0.03	-0.01
2.11	0.36	-0.09	0.04	0.12	-0.06	0.01	-0.08	0.06	-0.22	0.12	-0.03	0.07	0.03	-0.00
2.12	0.36	-0.10	0.03	0.12	-0.05	0.01	-0.08	0.06	-0.22	0.11	-0.03	0.07	0.02	-0.00
2.13	0.35	0.11	0.02	0.12	-0.05	0.01	-0.08	0.06	-0.23	0.10	-0.03	0.07	0.02	-0.00
2.14	0.35	0.12	0.01	0.13	-0.05	0.01	-0.09	0.06	-0.23	0.10	-0.03	0.07	0.02	-0.00
2.15	0.34	0.13	0.00	0.13	-0.05	0.01	-0.09	0.06	-0.24	0.09	-0.03	0.07	0.02	-0.00
2.16	0.34	0.13	-0.00	0.13	-0.05	0.01	-0.09	0.06	-0.24	0.08	-0.03	0.07	0.02	-0.00
2.17	0.34	0.14	-0.01	0.14	0.05	0.01	0.09	0.06	-0.24	0.07	-0.04	0.07	0.02	-0.00

Table 7 (continued)

1DD03		3FP05		1FF05		3FF05		1FF07		3GD07		1GG07		3GG07	
-0.02	0.01	0.06	0.12	0.00	0.00	0.00	0.00	-0.00	0.00	0.01	0.00	0.00	0.00	-0.00	0.00
0.03	0.01	0.06	0.13	0.00	0.00	0.00	0.00	-0.00	0.01	0.01	0.00	0.00	0.00	-0.00	0.00
-0.03	0.01	0.06	0.15	0.00	0.00	0.00	0.00	-0.00	0.01	0.01	0.00	0.00	0.00	-0.00	0.00
-0.03	0.02	0.06	0.16	0.00	0.00	0.00	0.00	-0.00	0.01	0.01	0.00	0.00	0.00	-0.00	0.01
-0.04	0.02	0.06	0.18	0.00	0.00	0.00	0.00	-0.01	0.01	0.02	0.00	0.00	0.00	-0.00	0.01
-0.05	0.02	0.06	0.19	0.01	0.00	0.00	0.00	-0.01	0.01	0.02	0.00	0.00	0.00	-0.01	0.01
-0.05	0.02	0.05	0.21	0.01	0.00	0.00	0.00	-0.01	0.01	0.03	0.01	0.00	0.00	-0.01	0.01
-0.06	0.03	0.05	0.22	0.01	0.00	0.00	0.00	-0.01	0.02	0.03	0.01	0.00	0.00	-0.01	0.01
-0.06	0.03	0.05	0.23	0.01	0.00	0.00	0.00	-0.01	0.02	0.04	0.01	0.00	0.00	-0.01	0.02
-0.07	0.03	0.04	0.24	0.01	0.00	0.00	0.00	-0.01	0.02	0.04	0.01	0.00	0.00	-0.01	0.02
-0.08	0.04	0.04	0.25	0.02	0.00	0.00	0.00	-0.02	0.03	0.05	0.02	0.00	0.00	-0.01	0.02
-0.08	0.04	0.03	0.26	0.02	0.01	0.00	0.00	-0.02	0.03	0.06	0.02	0.00	0.00	-0.02	0.03
-0.09	0.04	0.02	0.27	0.02	0.01	0.00	0.00	-0.02	0.04	0.06	0.03	0.00	0.00	-0.02	0.03
-0.09	0.04	0.02	0.27	0.03	0.01	0.00	0.00	-0.02	0.04	0.07	0.03	0.01	0.00	-0.02	0.04
-0.10	0.05	0.01	0.28	0.03	0.01	0.00	0.00	-0.02	0.04	0.08	0.04	0.01	0.00	-0.02	0.04
-0.11	0.05	0.00	0.28	0.04	0.02	0.00	0.00	-0.03	0.05	0.08	0.05	0.01	0.00	-0.03	0.04
-0.11	0.05	-0.01	0.28	0.04	0.02	0.00	0.00	-0.03	0.05	0.09	0.06	0.01	0.01	-0.03	0.05
-0.12	0.05	-0.01	0.28	0.05	0.02	0.00	0.00	-0.03	0.06	0.10	0.07	0.01	0.01	-0.03	0.05
-0.12	0.06	-0.02	0.28	0.05	0.03	0.00	0.00	-0.03	0.06	0.10	0.09	0.01	0.01	-0.03	0.05
-0.12	0.06	-0.03	0.28	0.06	0.04	0.00	0.00	-0.04	0.07	0.10	0.10	0.01	0.01	-0.04	0.06
-0.13	0.06	-0.04	0.28	0.06	0.05	0.00	0.00	-0.04	0.07	0.10	0.12	0.01	0.02	-0.04	0.06
-0.13	0.06	-0.04	0.28	0.07	0.06	0.01	0.00	-0.04	0.08	0.10	0.14	0.01	0.02	-0.04	0.06
-0.14	0.06	-0.05	0.28	0.07	0.07	0.01	0.01	-0.04	0.08	0.09	0.15	0.01	0.02	-0.04	0.06
-0.14	0.07	-0.06	0.28	0.07	0.08	0.01	0.01	-0.05	0.08	0.08	0.17	0.01	0.03	-0.04	0.07
-0.15	0.07	-0.07	0.27	0.07	0.10	0.01	0.01	-0.05	0.09	0.07	0.19	0.01	0.03	-0.04	0.07
-0.15	0.07	-0.07	0.27	0.07	0.12	0.01	0.01	-0.05	0.09	0.05	0.20	0.01	0.03	-0.04	0.06
-0.15	0.07	-0.08	0.27	0.06	0.13	0.00	0.01	-0.05	0.10	0.04	0.21	0.01	0.04	-0.04	0.06
-0.16	0.07	-0.09	0.26	0.05	0.15	0.00	0.01	-0.06	0.10	0.02	0.21	0.00	0.04	-0.04	0.06
-0.16	0.08	-0.10	0.25	0.03	0.16	0.00	0.01	-0.06	0.11	0.00	0.21	0.00	0.04	-0.04	0.06
-0.16	0.08	-0.10	0.25	0.01	0.17	0.00	0.01	-0.06	0.11	-0.02	0.21	-0.00	0.04	-0.03	0.05
-0.17	0.08	-0.11	0.24	-0.01	0.18	-0.00	0.01	-0.06	0.11	-0.03	0.21	-0.01	0.05	-0.03	0.05
-0.17	0.08	-0.12	0.23	-0.03	0.17	-0.00	0.01	-0.06	0.12	-0.04	0.20	-0.01	0.05	-0.03	0.04
-0.17	0.08	-0.12	0.22	-0.05	0.17	-0.00	0.01	-0.07	0.12	-0.06	0.20	-0.01	0.05	-0.02	0.03
-0.17	0.08	-0.12	0.21	-0.06	0.16	-0.01	0.01	-0.07	0.13	-0.07	0.19	-0.02	0.05	-0.02	0.02
-0.18	0.08	-0.13	0.20	-0.08	0.15	-0.01	0.01	-0.07	0.13	-0.07	0.18	-0.02	0.05	-0.01	0.01

Table 7 (continued)

Ecm	1SS11	3SD11	1PP11	3PP11	1PP13	3PP13	3DS13	1DD13	3DD13
1.83	-0.02 0.07	0.01 -0.03	0.03 0.02	0.03 0.03	0.02 0.01	-0.03 0.01	-0.02 0.01	-0.01 -0.01	-0.02 -0.00
1.84	-0.02 0.07	0.02 -0.03	0.03 0.03	0.03 0.05	0.02 -0.01	-0.03 0.01	-0.02 -0.02	0.01 -0.01	0.02 -0.01
1.85	-0.02 0.07	0.03 -0.02	0.03 0.04	0.02 0.07	0.03 -0.01	-0.03 0.01	-0.02 -0.02	0.01 -0.01	-0.02 -0.01
1.86	-0.02 0.06	0.03 -0.02	0.02 0.05	0.01 0.09	0.03 -0.01	-0.04 0.01	-0.02 -0.03	-0.01 -0.02	-0.02 0.01
1.87	0.02 0.06	0.03 -0.01	0.01 0.05	-0.02 0.10	0.03 -0.01	0.04 0.01	-0.02 -0.04	-0.01 -0.02	-0.03 -0.01
1.88	-0.02 0.05	0.03 0.00	-0.00 0.06	-0.05 0.10	0.04 -0.01	-0.04 0.01	-0.02 -0.05	-0.01 -0.03	-0.03 -0.02
1.89	-0.02 0.04	0.03 0.01	-0.01 0.05	-0.08 0.09	0.04 -0.01	-0.05 0.01	-0.01 -0.06	-0.01 -0.03	-0.03 -0.02
1.90	-0.02 0.03	0.01 0.02	-0.01 0.05	-0.09 0.07	0.04 -0.02	-0.05 0.01	-0.00 -0.06	-0.01 -0.04	-0.03 -0.02
1.91	-0.02 0.02	-0.00 0.02	-0.02 0.04	-0.10 0.06	0.04 -0.02	-0.05 0.01	0.01 -0.07	-0.01 -0.04	-0.03 -0.03
1.92	-0.01 0.00	-0.02 0.02	-0.02 0.03	-0.10 0.04	0.05 -0.02	-0.06 0.01	0.02 -0.07	-0.01 -0.05	-0.03 -0.03
1.93	-0.00 -0.01	-0.03 0.01	-0.02 0.03	-0.10 0.03	0.05 -0.02	-0.06 0.01	0.03 -0.07	-0.01 -0.05	-0.03 -0.03
1.94	0.01 -0.02	-0.04 -0.00	-0.01 0.03	-0.10 0.02	0.05 -0.02	-0.06 0.02	0.04 -0.07	-0.00 -0.05	-0.03 -0.03
1.95	0.02 -0.03	-0.05 -0.02	-0.01 0.02	-0.10 0.02	0.05 -0.02	-0.06 0.02	0.05 -0.06	0.00 -0.05	-0.03 -0.03
1.96	0.03 -0.03	-0.05 -0.04	-0.01 0.02	-0.10 0.01	0.05 -0.02	-0.07 0.02	0.06 -0.06	0.00 -0.05	-0.03 0.03
1.97	0.04 -0.04	-0.05 -0.06	-0.01 0.02	-0.10 0.01	0.05 -0.02	-0.07 0.02	0.06 -0.05	0.01 -0.05	-0.03 -0.03
1.98	0.05 -0.04	0.04 -0.07	-0.01 0.02	-0.10 0.00	0.06 -0.02	-0.07 0.02	0.07 -0.04	0.01 -0.05	-0.03 -0.03
1.99	0.05 -0.04	-0.03 -0.09	-0.01 0.02	-0.10 0.00	0.06 -0.02	-0.07 0.02	0.07 -0.04	0.01 -0.05	-0.03 -0.02
2.00	0.06 -0.04	-0.02 -0.10	-0.00 0.02	-0.09 -0.00	0.06 -0.02	-0.07 0.02	0.07 -0.03	0.01 -0.05	-0.03 -0.02
2.01	0.06 -0.04	0.00 -0.10	-0.00 0.02	-0.09 -0.01	0.06 -0.02	-0.08 0.02	0.08 -0.03	0.01 -0.05	-0.04 -0.02
2.02	0.06 -0.04	0.02 -0.10	-0.00 0.02	-0.09 -0.01	0.06 -0.02	-0.08 0.02	0.08 -0.02	0.01 -0.05	-0.04 -0.02
2.03	0.06 -0.04	0.04 -0.10	-0.00 0.02	-0.09 -0.01	0.06 -0.02	-0.08 0.02	0.08 -0.02	0.01 -0.05	-0.04 -0.02
2.04	0.06 -0.04	0.05 -0.09	0.00 0.02	-0.09 -0.01	0.06 -0.02	-0.08 0.02	0.08 -0.01	0.01 -0.05	-0.04 -0.02
2.05	0.06 -0.04	0.06 -0.08	0.00 0.02	-0.09 -0.01	0.06 -0.02	-0.08 0.02	0.08 -0.01	0.01 -0.05	-0.04 -0.02
2.06	0.05 -0.04	0.06 -0.06	0.00 0.02	-0.09 -0.01	0.07 -0.02	-0.08 0.02	0.08 -0.01	0.01 -0.05	-0.04 -0.01
2.07	0.05 -0.05	0.06 -0.05	0.00 0.02	-0.09 -0.01	0.07 -0.02	-0.08 0.02	0.08 -0.00	0.01 -0.05	-0.05 -0.01
2.08	0.05 -0.05	0.05 -0.04	0.00 0.02	-0.09 -0.02	0.07 -0.03	-0.09 0.02	0.08 0.00	0.01 -0.05	-0.05 -0.01
2.09	0.04 -0.05	0.05 -0.03	0.00 0.02	-0.09 -0.02	0.07 -0.03	-0.09 0.02	0.08 0.00	0.01 -0.05	-0.05 -0.01
2.10	0.04 -0.06	0.04 -0.03	0.01 0.02	-0.08 -0.02	0.07 -0.03	-0.09 0.02	0.07 0.01	0.01 -0.05	-0.05 -0.01
2.11	0.03 -0.06	0.03 -0.04	0.01 0.02	-0.08 -0.02	0.07 -0.03	-0.09 0.02	0.07 0.01	0.00 -0.05	-0.05 -0.01
2.12	0.02 -0.06	0.02 -0.04	0.01 0.02	-0.08 -0.02	0.07 -0.03	-0.09 0.02	0.07 0.01	0.00 -0.05	-0.06 -0.01
2.13	0.02 -0.07	0.02 -0.06	0.01 0.02	-0.08 -0.02	0.07 -0.03	-0.09 0.02	0.07 0.01	0.00 -0.05	-0.06 -0.01
2.14	0.01 -0.07	0.02 -0.07	0.01 0.02	-0.08 -0.02	0.07 -0.03	-0.09 0.02	0.07 0.01	0.00 -0.05	-0.06 -0.01
2.15	0.00 -0.08	0.03 -0.08	0.01 0.02	-0.08 -0.02	0.07 -0.03	-0.09 0.02	0.07 0.01	0.00 -0.05	-0.06 -0.01
2.16	0.00 -0.08	0.05 -0.10	0.01 0.02	-0.08 -0.02	0.07 -0.03	-0.09 0.02	0.07 0.02	0.00 -0.05	-0.06 -0.01
2.17	0.01 -0.09	0.07 -0.10	0.01 0.02	-0.08 0.02	0.08 -0.03	-0.09 0.02	0.07 0.02	0.00 -0.05	-0.06 -0.01

Table 7 (continued)

1DD15	3DD15	3FP15	1FF15	3FF15	1FF17	3FF17	3FH17	3GD17	3GG17
0.01 -0.01	-0.03 0.01	-0.01 -0.00	0.00 0.00	0.00 0.00	-0.00 -0.00	0.00 0.00	0.00 0.00	0.00 -0.00	-0.00 0.00
0.01 -0.01	-0.03 0.01	-0.01 -0.00	0.00 0.00	0.00 0.00	-0.00 -0.00	0.00 0.00	0.00 0.00	0.00 -0.00	-0.00 0.00
0.01 -0.01	-0.04 0.01	-0.01 -0.01	0.00 0.00	0.00 0.00	-0.00 -0.00	0.00 0.00	0.00 0.00	0.00 -0.00	-0.00 0.00
0.02 -0.01	-0.04 0.01	-0.01 -0.01	0.00 0.00	0.01 0.00	-0.00 -0.00	0.00 0.00	0.00 0.00	0.00 -0.00	-0.00 0.00
0.02 -0.01	-0.05 0.01	-0.01 -0.01	0.00 0.00	0.01 0.01	-0.00 -0.00	0.00 0.00	0.00 0.00	0.00 -0.00	-0.00 0.00
0.02 -0.01	-0.05 0.00	-0.01 -0.02	0.00 0.00	0.01 0.01	-0.00 -0.00	0.00 0.00	0.00 0.00	0.01 -0.00	-0.00 0.00
0.03 -0.01	0.06 0.00	-0.01 -0.02	0.00 0.01	0.01 0.01	-0.01 -0.00	0.00 0.00	0.00 0.00	0.01 -0.00	-0.00 0.00
0.03 -0.01	-0.06 0.00	-0.01 -0.02	0.00 0.01	0.01 0.02	-0.01 -0.00	0.01 0.00	0.00 0.00	0.01 -0.00	-0.00 0.00
0.03 -0.02	-0.07 0.00	-0.00 -0.03	0.00 0.01	0.00 0.02	-0.01 -0.00	0.01 0.00	0.00 0.00	0.01 -0.00	-0.00 0.00
0.04 -0.02	-0.07 0.00	-0.00 -0.03	0.00 0.01	0.00 0.03	-0.01 -0.01	0.01 0.00	0.00 0.00	0.01 -0.00	-0.00 0.00
0.04 -0.02	-0.08 0.00	0.00 -0.03	-0.00 0.01	-0.00 0.03	-0.01 -0.01	0.01 0.01	0.00 0.00	0.01 -0.00	-0.00 0.00
0.04 -0.02	-0.08 -0.00	0.01 -0.03	-0.00 0.01	-0.01 0.03	-0.01 -0.01	0.01 0.01	0.00 0.00	0.01 -0.01	-0.01 0.00
0.05 -0.02	-0.09 -0.00	0.01 -0.02	-0.00 0.01	-0.01 0.03	-0.02 -0.01	0.01 0.01	0.00 0.00	0.01 -0.01	-0.01 0.00
0.05 -0.02	-0.09 -0.00	0.01 -0.02	-0.01 0.01	-0.02 0.03	-0.02 -0.02	0.01 0.01	0.01 0.01	0.01 -0.01	-0.01 0.00
0.05 -0.03	-0.09 -0.01	0.01 -0.02	-0.01 0.01	-0.02 0.03	-0.02 -0.02	0.01 0.02	0.01 0.01	0.02 -0.01	-0.01 0.00
0.05 -0.03	-0.10 -0.01	0.01 -0.02	-0.01 0.01	-0.02 0.03	-0.02 -0.03	0.01 0.02	0.01 0.01	0.02 -0.01	-0.01 0.00
0.06 -0.03	-0.10 -0.01	0.02 -0.02	-0.01 0.01	-0.02 0.03	-0.02 -0.03	0.01 0.03	0.01 0.01	0.02 -0.01	-0.01 0.00
0.06 -0.03	-0.10 -0.01	0.02 -0.02	-0.01 0.01	-0.03 0.03	-0.02 -0.04	0.01 0.03	0.01 0.01	0.02 -0.01	-0.01 0.01
0.06 -0.03	-0.10 -0.01	0.02 -0.01	-0.01 0.01	-0.03 0.02	-0.02 -0.05	0.01 0.03	0.01 0.02	0.02 -0.01	-0.02 0.01
0.06 -0.03	-0.10 -0.02	0.02 -0.01	-0.01 0.01	-0.03 0.02	-0.01 -0.05	0.01 0.04	0.00 0.02	0.02 -0.01	-0.02 0.01
0.07 -0.03	-0.10 -0.02	0.02 -0.01	-0.01 0.01	-0.03 0.02	-0.01 -0.05	0.00 0.04	0.00 0.02	0.02 -0.01	-0.02 0.01
0.07 -0.03	-0.10 -0.02	0.02 -0.01	-0.01 0.01	-0.03 0.02	-0.00 -0.06	0.00 0.04	0.00 0.02	0.02 -0.01	-0.02 0.01
0.07 -0.04	-0.10 -0.02	0.01 -0.01	-0.01 0.01	-0.03 0.02	0.01 -0.06	-0.00 0.04	-0.00 0.02	0.02 -0.01	-0.02 0.01
0.07 -0.04	-0.10 -0.02	0.01 -0.01	-0.01 0.01	-0.03 0.02	0.01 -0.06	-0.01 0.05	-0.00 0.02	0.02 -0.01	-0.03 0.01
0.07 -0.04	-0.10 -0.02	0.01 -0.01	-0.01 0.01	-0.03 0.02	0.02 -0.06	-0.01 0.04	-0.01 0.02	0.03 -0.01	-0.03 0.01
0.08 -0.04	-0.10 -0.03	0.01 -0.01	-0.01 0.01	-0.03 0.02	0.02 -0.06	-0.02 0.04	-0.01 0.02	0.03 -0.01	-0.03 0.01
0.08 -0.04	-0.10 -0.03	0.01 -0.01	-0.01 0.01	-0.03 0.02	0.03 -0.06	-0.02 0.04	-0.01 0.02	0.03 -0.01	-0.03 0.01
0.08 -0.04	-0.09 -0.03	0.01 -0.01	-0.01 0.01	-0.03 0.02	0.03 -0.05	-0.02 0.04	-0.01 0.02	0.03 -0.01	-0.04 0.01
0.08 -0.04	-0.09 -0.03	0.01 -0.01	-0.01 0.01	-0.03 0.02	0.03 -0.05	-0.02 0.04	-0.01 0.02	0.03 -0.01	-0.04 0.02
0.08 -0.04	-0.09 -0.03	0.01 -0.01	-0.01 0.01	-0.03 0.02	0.04 -0.05	-0.03 0.04	-0.02 0.02	0.03 -0.01	-0.04 0.02
0.08 -0.04	-0.09 -0.03	0.01 -0.01	-0.01 0.01	-0.03 0.02	0.04 -0.05	-0.03 0.03	-0.02 0.02	0.03 -0.01	-0.04 0.02
0.09 -0.04	-0.08 -0.03	0.01 -0.01	-0.01 0.01	-0.03 0.01	0.04 -0.04	-0.03 0.03	-0.02 0.02	0.03 -0.01	-0.05 0.02
0.09 -0.04	-0.08 -0.03	0.01 -0.01	-0.01 0.01	-0.03 0.01	0.04 -0.04	-0.03 0.03	-0.02 0.02	0.03 -0.01	-0.05 0.02
0.09 -0.04	-0.08 -0.03	0.01 -0.01	-0.01 0.01	-0.03 0.01	0.04 -0.04	-0.03 0.03	-0.02 0.02	0.03 -0.02	-0.05 0.02
0.09 -0.05	-0.08 -0.03	0.01 -0.01	-0.01 0.01	-0.03 0.01	0.04 -0.04	-0.03 0.03	-0.02 0.02	0.04 -0.02	-0.06 0.02

The waves are labelled by $2S'LL'I2J$: (a) $I = 0$ partial waves: waves 3DS03, 3DD03, 3DD05, 1DD05, 3DG05, 3FF07 and 3FH07 are identically zero everywhere; (b) $I = 1$ partial waves: waves 3PF13, 3DG15 and 1GG17 are identically zero everywhere.

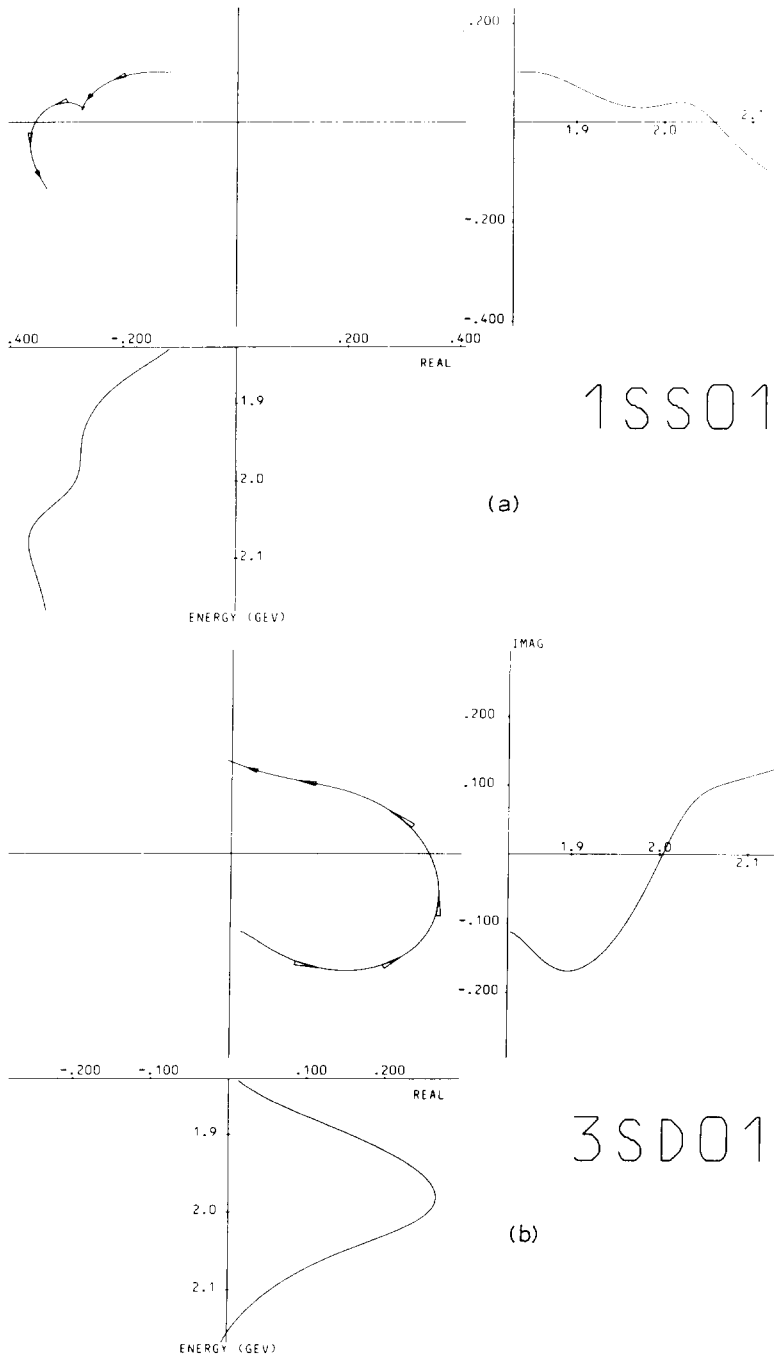

Fig. 5. Argand diagrams for some of the active partial waves.

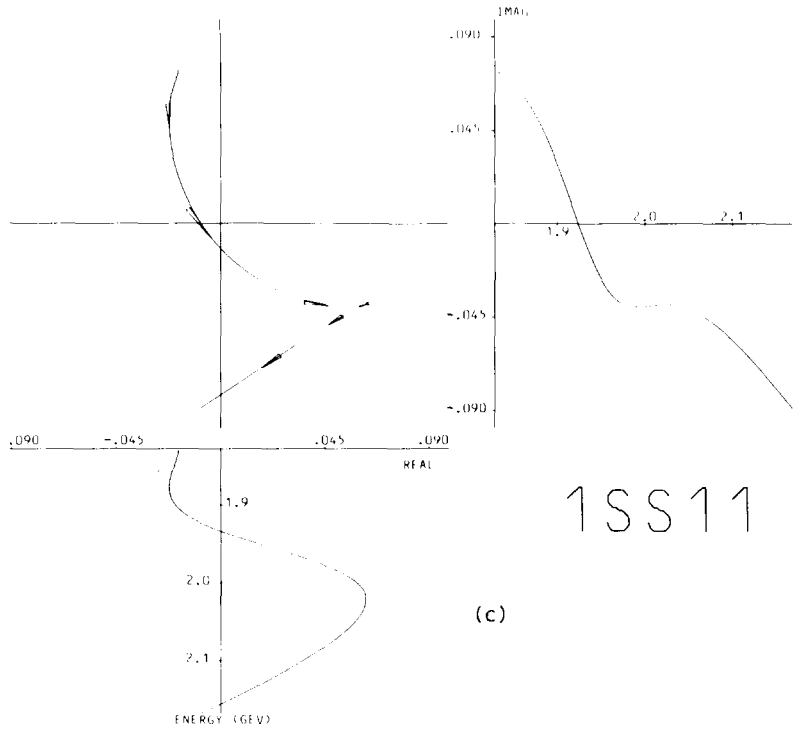

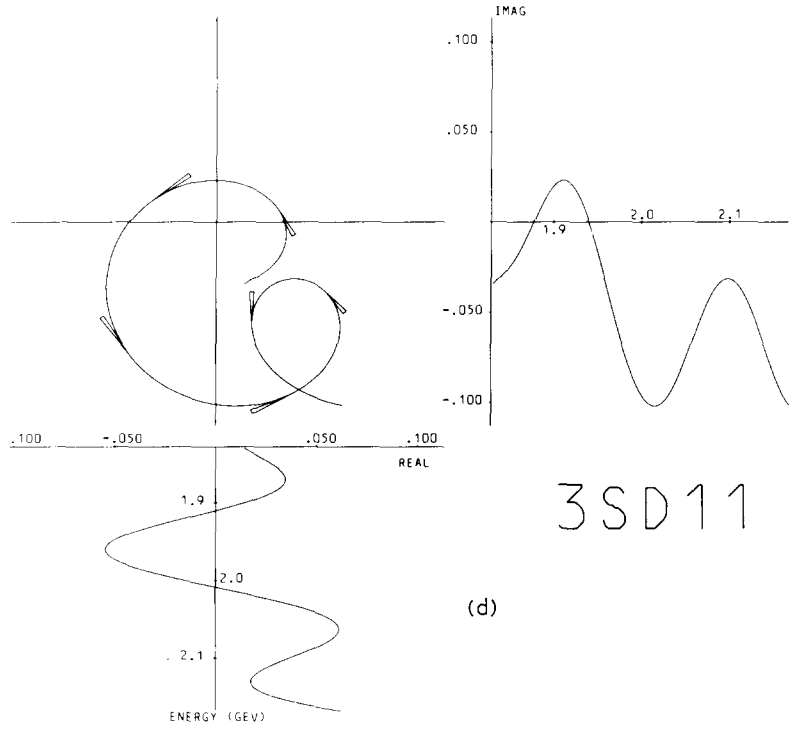

Fig. 5 (continued).

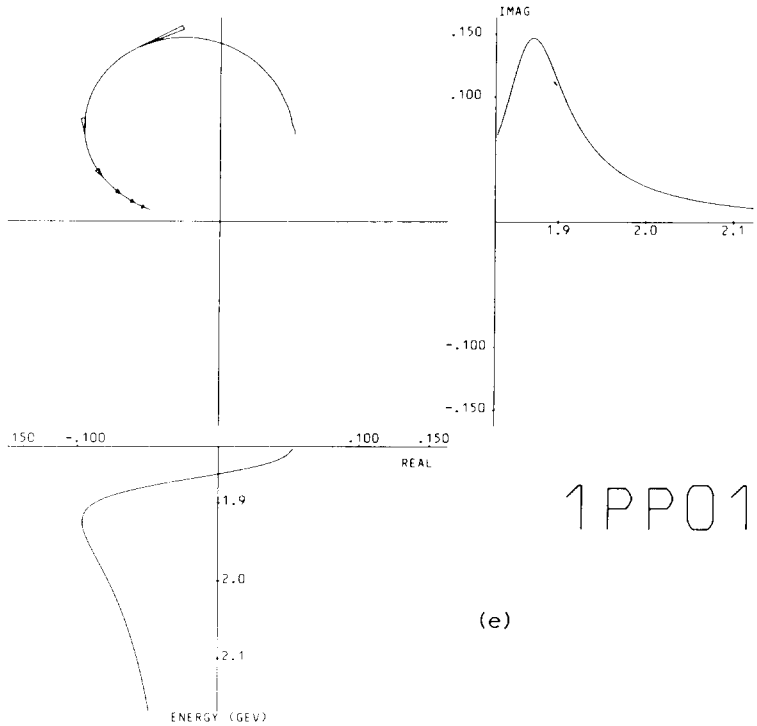

(e)

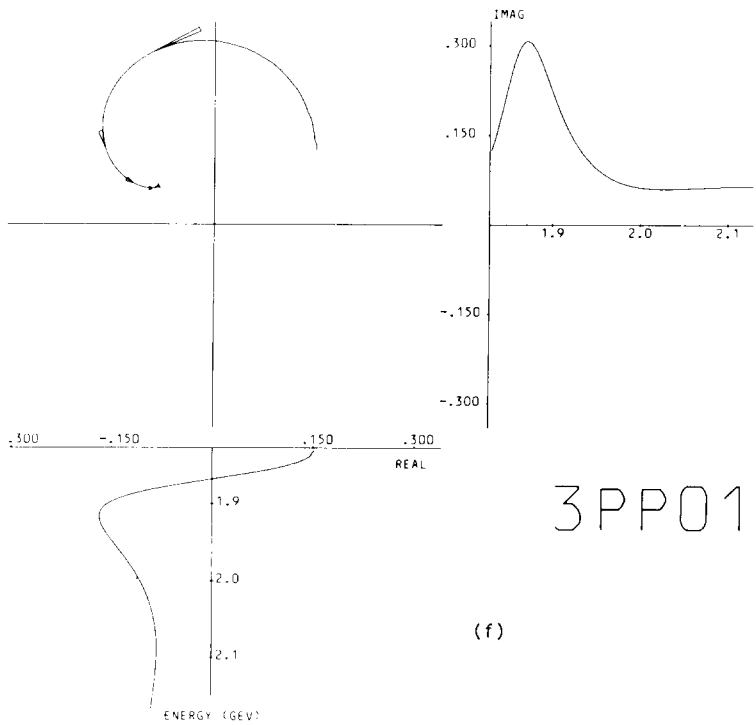

(f)

Fig. 5 (continued).

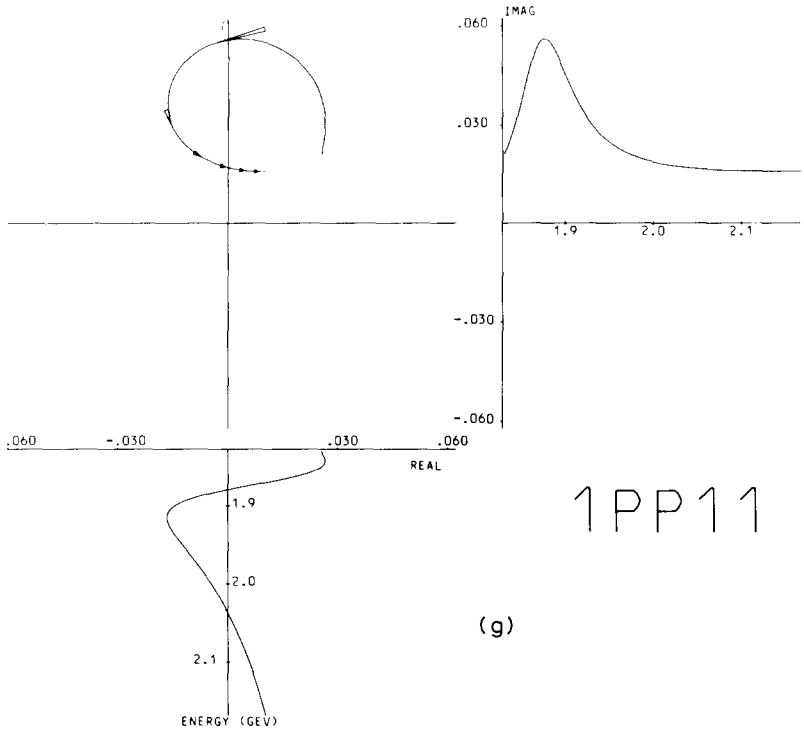

(g)

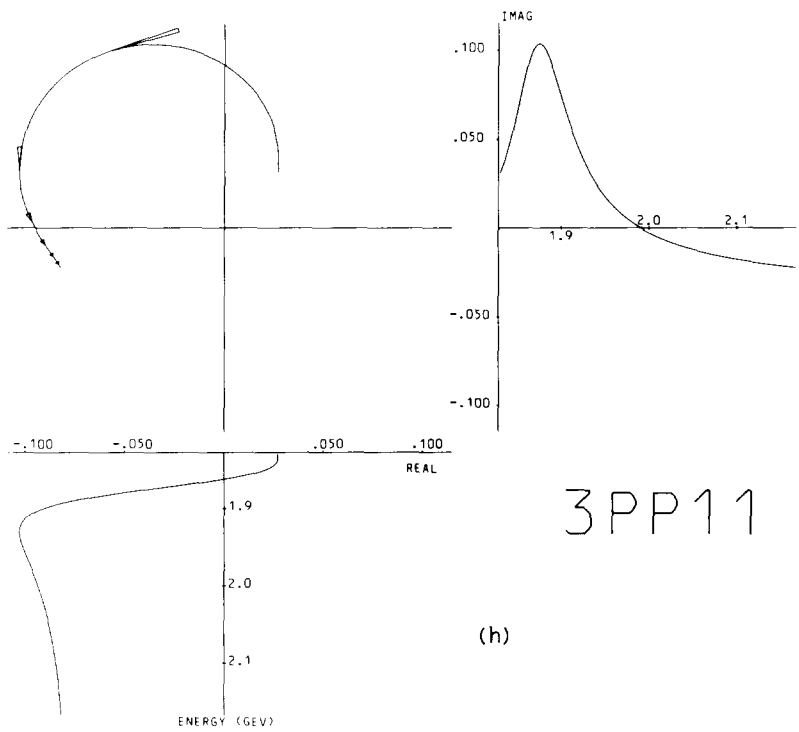

(h)

Fig. 5 (continued).

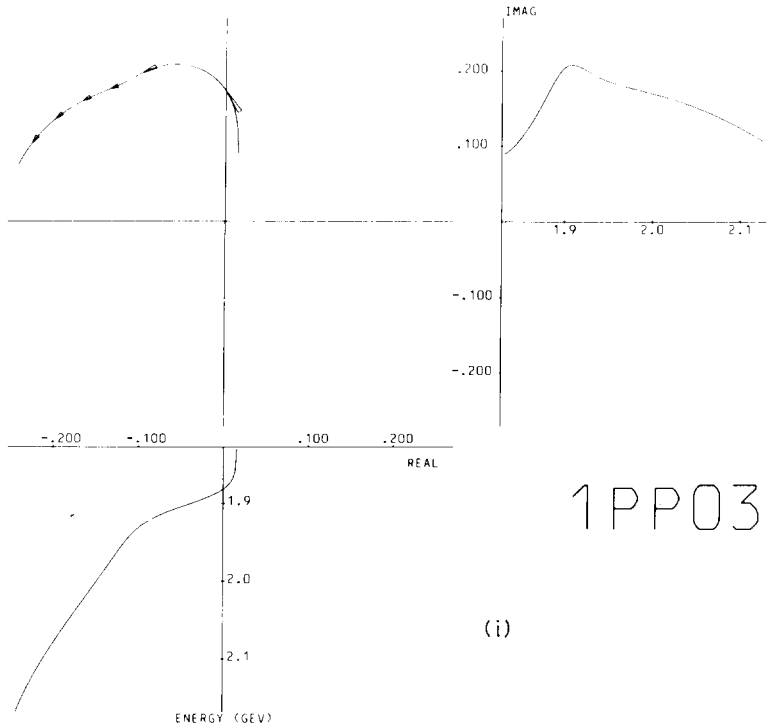

(i)

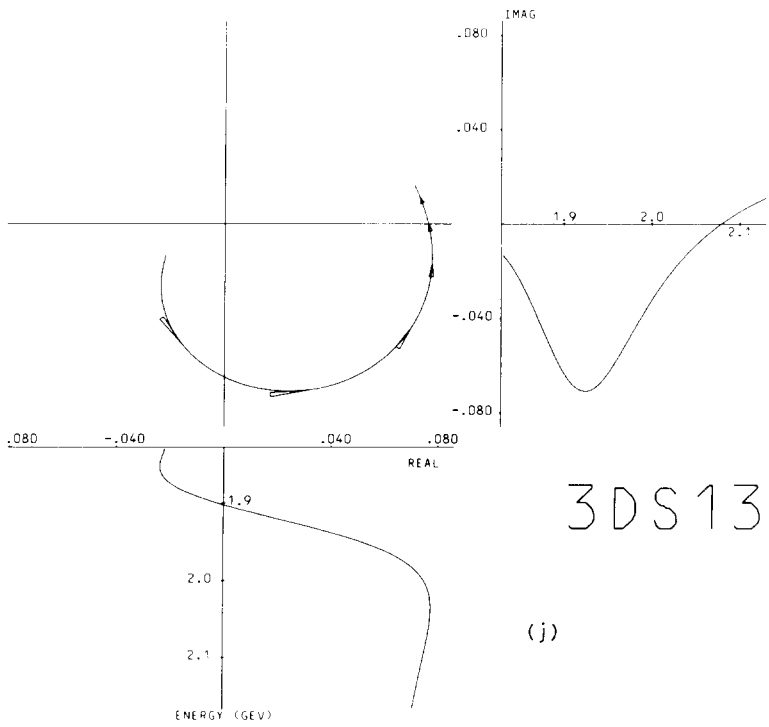

(j)

Fig. 5 (continued).

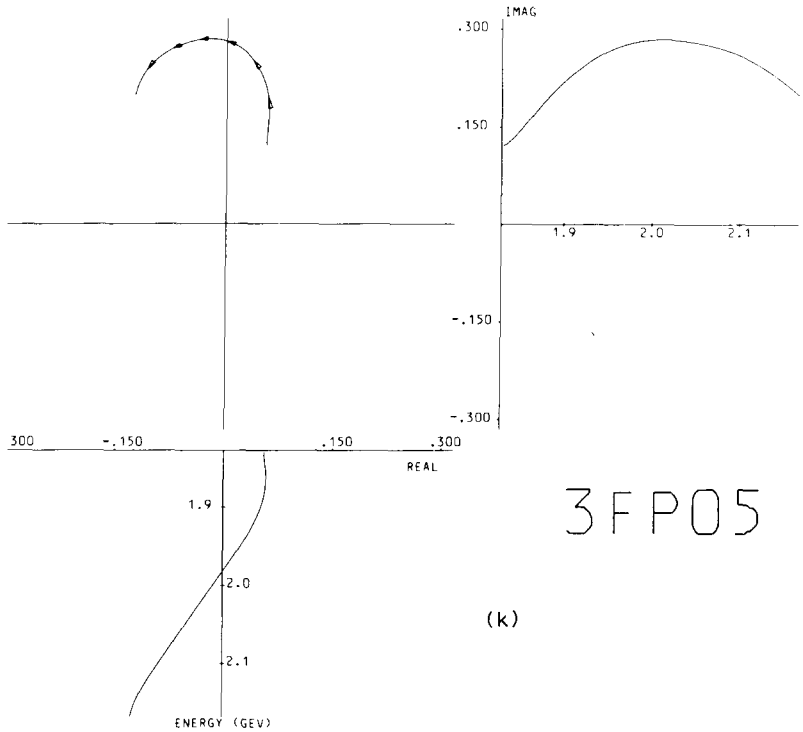

(k)

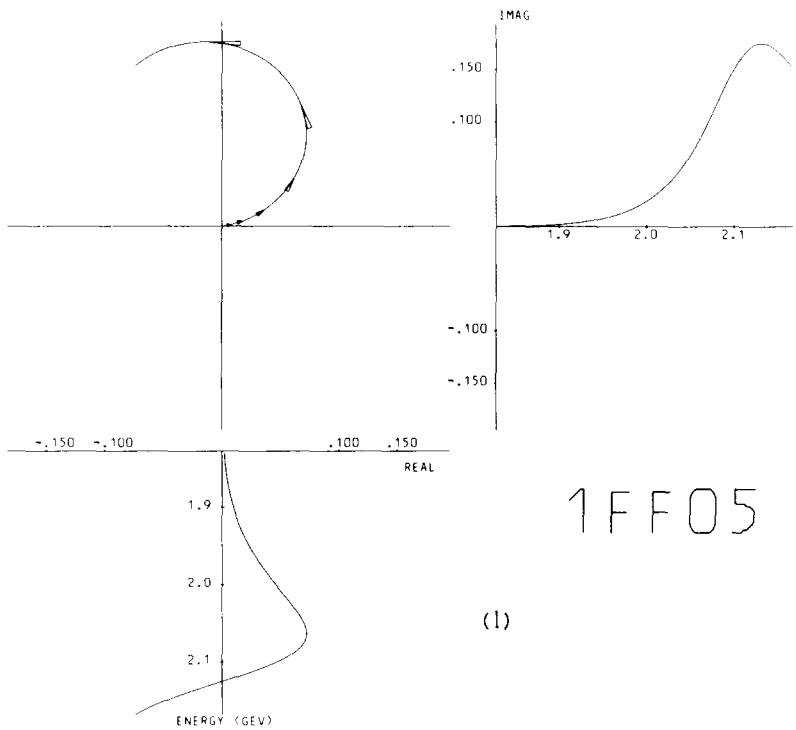

(l)

Fig. 5 (continued).

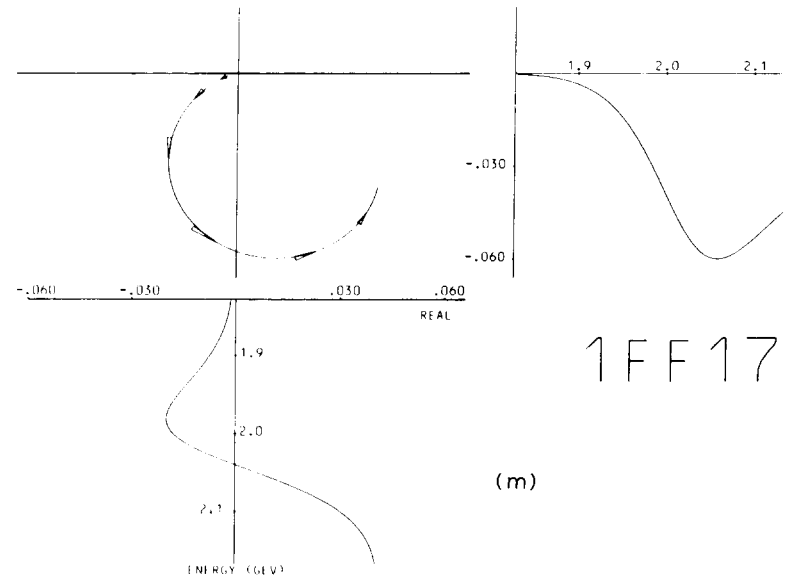

(m)

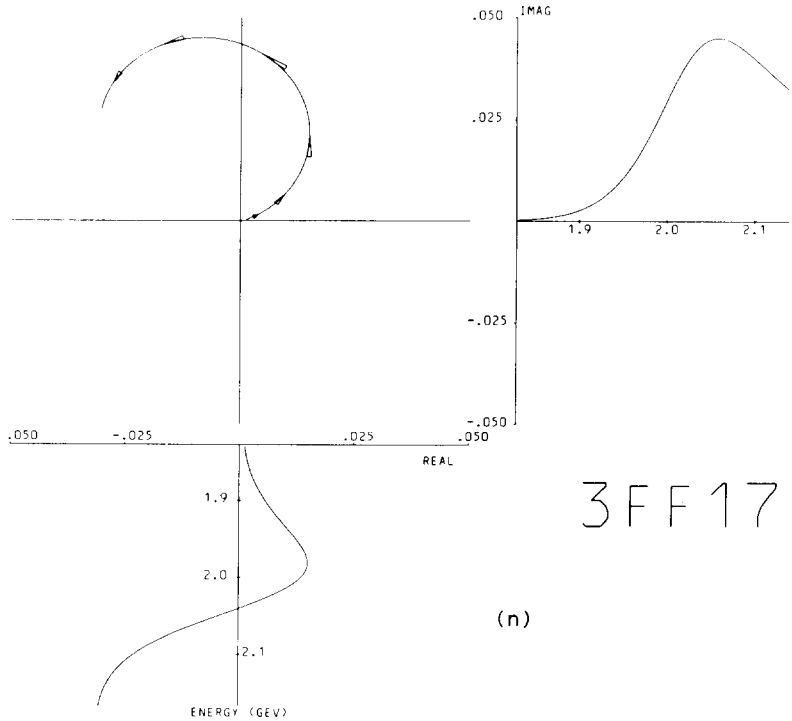

(n)

Fig. 5 (continued).

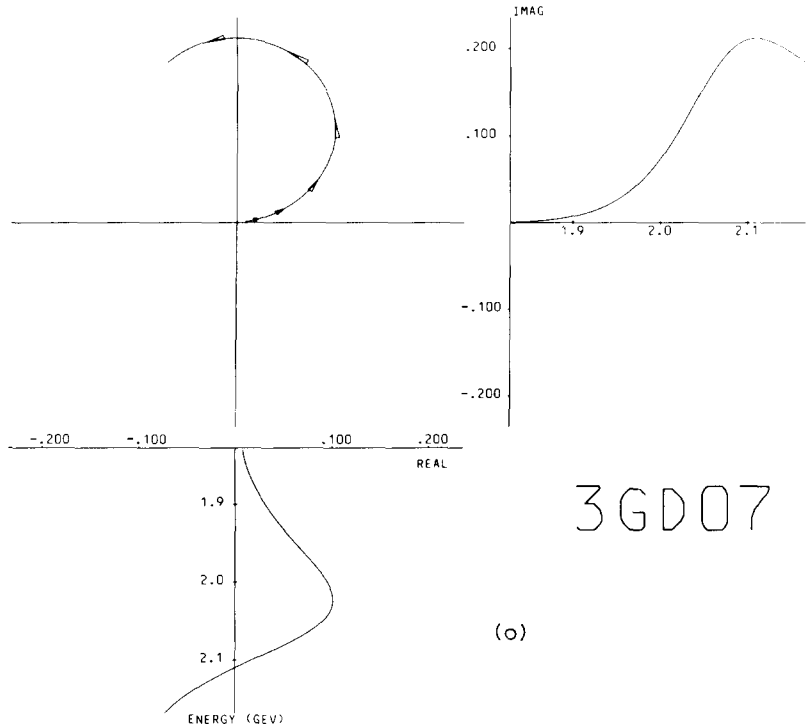

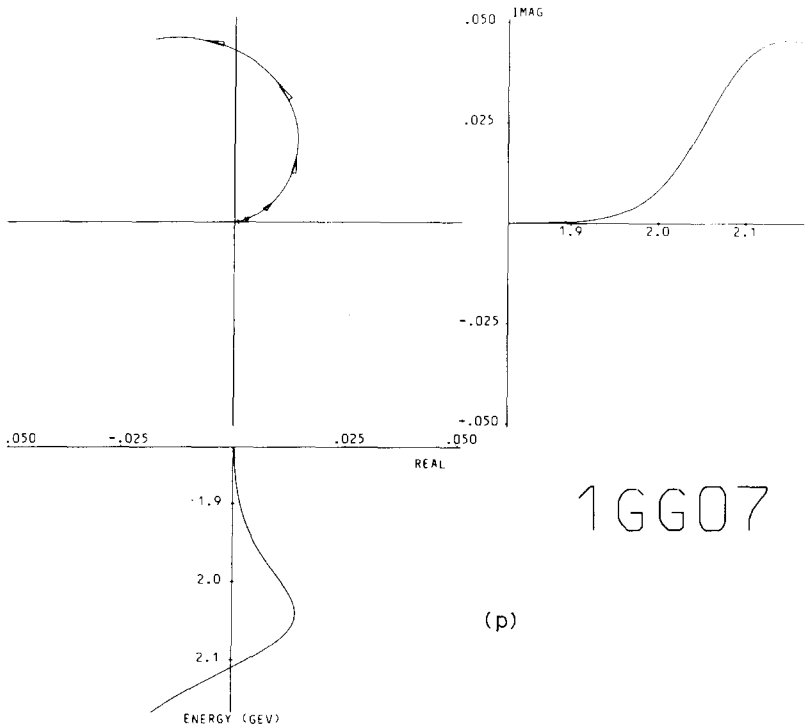

Fig. 5 (continued).

5. Summary and conclusions

Over the c.m. energy range 1775 to 1960 MeV each of the three single pion production channels $\overline{K^0}\pi^-p$, $K^-\pi^+n$ and $K^-p\pi^0$ is well-explained by incoherent quasi-two-body processes together with a small amount of non-interfering three-particle Lorentz invariant phase space. Production of the $\overline{K^*}(890)$ is found to be the dominant process above 1830 MeV. Using data well above the threshold for K^* production new values have been obtained for the masses and widths of the $\overline{K^{*0}}$ and K^{*-}. Data from this and earlier experiments have been used to determine the partial-wave amplitudes for $\bar{K}N \to \overline{K^*}(890)N$ from threshold to 2170 MeV. These, in general, give a good description of the data in all three charge states $\overline{K^{*0}}n$, $K^{*-}p$ and $K^{*-}n$.

Almost all the expected Y^* resonances [16] with masses above threshold are found to have strong couplings to this channel. New values have been determined for the masses and widths for some of these resonances. All these states have been assigned to high supermultiplets of SU(6) × O(3) [19] except the new S01(2030) state which presumably is a radial excitation state (e.g. of the $[70, 1^-]_3$).

It should be stressed that we have determined more significant couplings for the vector meson decays $Y^* \to \overline{K^*}N$ than has been possible in the corresponding ρN decays of non-strange baryons. Therefore, these results should provide critical constraints for higher symmetry decay schemes.

Three of us (R.W.M.H., P.N. and R.A.S.) are grateful to the Science Research Council for financial support.

References

[1] A. Berthon, G. Tristram, J. Vrana, T.C. Bacon, A.A. Brandstetter, I. Butterworth, G.P. Gopal, P.S. Jones, P.J. Litchfield, M. Mandelkern, J. Meyer, G. Poulard, B. Tallini, W. Wojcik, Z. Zatz and R. Strub, Nuovo Cim. 21A (1974) 146.

[2] M.J. Corden, G.F. Cox, I.R. Kenyon, S.W. O'Neale, J.A. Stubbs, K.C.T.O. Sumorok and P.M. Watkins, Nucl. Phys. B121 (1977) 365.

[3] RL-IC Collaboration, B. Conforto, G.P. Gopal, G.E. Kalmus, P.J. Litchfield, R.T. Ross, A.J. Van Horn, T.C. Bacon, I. Butterworth, E.F. Clayton and R.M. Waters, Nucl. Phys. B105 (1976) 189.

[4] Particle Data Group, Rev. Mod. Phys. 48 (1976) 1.

[5] J.C. Doyle, PhD thesis, University of California, UCRL 18139 (1969).

[6] P. Newham, PhD thesis, Imperial College, London, issued as Rutherford Laboratory report HEP/T/66 (1977).

[7] A. de Bellefon, A. Berthon, L.K. Rangan, J. Vrana, T.C. Bacon, A. Brandstetter, I. Butterworth, S.M. Deen, C.M. Fisher, P.J. Litchfield, R.J. Miller, J.R. Smith, G. Burgun, J. Meyer, E. Pauli, G. Poulard, B. Tallini, W. Wojcik, J. Zatz and R. Strub, Nuovo Cim. 7A (1972) 567.

[8] D. Merrill, W. Barletta, B. Conforto, D. Harmsen, T. Lasinski, R. Levi Setti, E. Burkhardt and H. Oberlack, Nucl. Phys. B60 (1973) 315.

[9] RL-IC Collaboration, W. Cameron, B. Franek, G.P. Gopal, G.E. Kalmus, A.C. McPherson, R.T. Ross, D.H. Saxon, T.C. Bacon, I. Butterworth, R.W.M. Hughes, P. Newham and R.A. Stern, Nucl. Phys. B131 (1977) 399.
[10] J.D. Jackson, Nuovo Cim. 34 (1974) 1644.
[11] A. De Rújula, H. Georgi and S.L. Glashow, Phys. Rev. D12 (1975) 147.
[12] B. Franek, Rutherford Laboratory report RL 77-069/A.
[13] S.M. Deen, Rutherford Laboratory preprint RPP/H/68.
[14] J.M. Blatt and V.F. Weisskopf, Theoretical nuclear physics (Wiley, New York, 1952) p. 361.
[15] B. Franek, Rutherford Laboratory, bubble chamber group physics note no. 110, unpublished.
[16] RL-IC Collaboration, G.P. Gopal, R.T. Ross, A.J. Van Horn, A.C. McPherson, E.F. Clayton, T.C. Bacon and I. Butterworth, Nucl. Phys. B119 (1977) 362.
[17] A. Lea, B. Martin, R. Moorhouse and G. Oades, Nucl. Phys. B56 (1973) 77.
[18] P.N. Hansen, J. Moss and G.C. Oades, Contribution to Oxford Baryon Conf. 1976, Conf. Proc. p. 275.
[19] M. Jones, R.H. Dalitz and R.R. Horgan, Nucl. Phys. B129 (1977) 45;
P.J. Litchfield, R.J. Cashmore and A.J.G. Hey, Rutherford Laboratory report RL-76-11.